

AD-A071 370

PHYSICS INTERNATIONAL CO SAN LEANDRO CALIF

F/G 11/4

SURFACE CONDITIONING OF CARBON PHENOLIC SPECIMENS BY PULSED ELE--ETC(U)

DNA001-77-C-0193

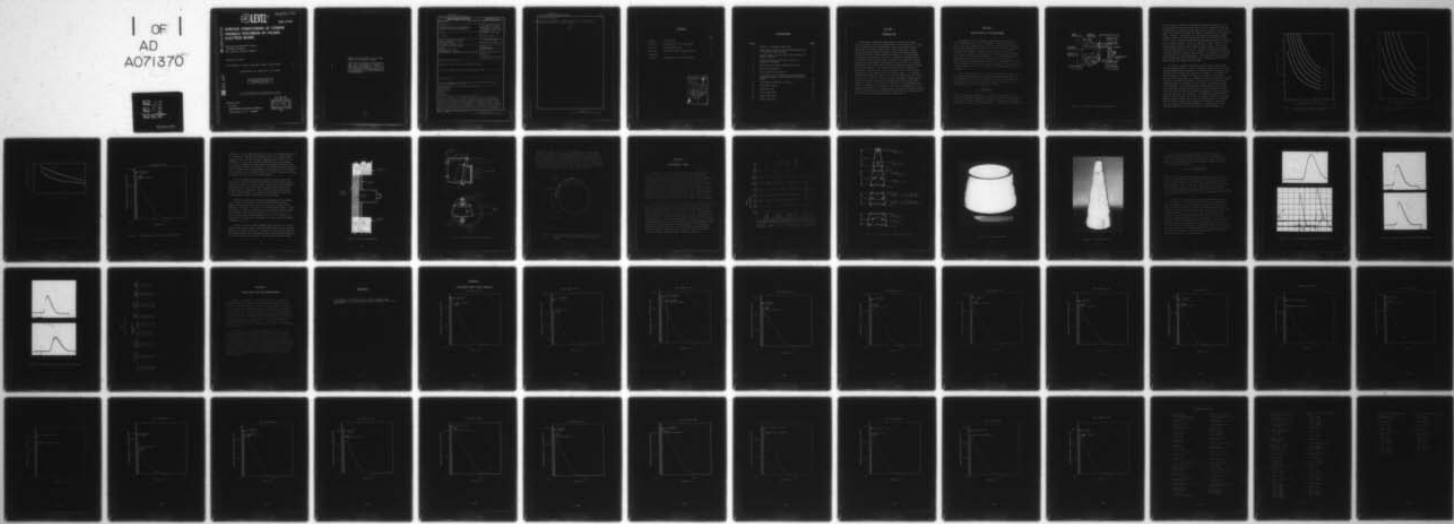
SEP 78 K TRIEBES

NL

UNCLASSIFIED

PIFR-1050-2

DNA-4703F



END  
DATE  
FILED

8-79  
DDC

(12) LEVEL III

AD-E300527

A059941

DNA 4703F

AD A 071370 SURFACE CONDITIONING OF CARBON  
PHENOLIC SPECIMENS BY PULSED  
ELECTRON BEAMS

Physics International Company  
2700 Merced Street  
San Leandro, California 94577

September 1978

Final Report for Period 22 May 1978-1 June 1978

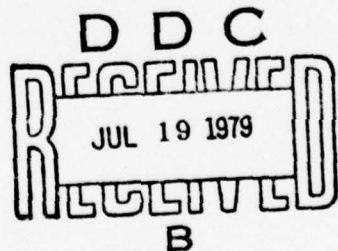
CONTRACT No. DNA 001-77-C-0193

DDC FILE COPY

APPROVED FOR PUBLIC RELEASE;  
DISTRIBUTION UNLIMITED.

THIS WORK SPONSORED BY THE DEFENSE NUCLEAR AGENCY  
UNDER RDT&E RMSS CODE B342077464 N99QAXAK11207 H2590D.

Prepared for  
Director  
DEFENSE NUCLEAR AGENCY  
Washington, D. C. 20305



Destroy this report when it is no longer  
needed. Do not return to sender.

[  
PLEASE NOTIFY THE DEFENSE NUCLEAR AGENCY,  
ATTN: TISI, WASHINGTON, D.C. 20305, IF  
YOUR ADDRESS IS INCORRECT, IF YOU WISH TO  
BE DELETED FROM THE DISTRIBUTION LIST, OR  
IF THE ADDRESSEE IS NO LONGER EMPLOYED BY  
YOUR ORGANIZATION.



## UNCLASSIFIED

SECURITY CLASSIFICATION OF THIS PAGE (When Data Entered)

REPORT DOCUMENTATION PAGE		READ INSTRUCTIONS BEFORE COMPLETING FORM
1. REPORT NUMBER DNA 4703F	2. GOVT ACCESSION NO.	3. RECIPIENT'S CATALOG NUMBER
4. TITLE (and Subtitle)  SURFACE CONDITIONING OF CARBON PHENOLIC SPECIMENS BY PULSED ELECTRON BEAMS		5. TYPE OF REPORT & PERIOD COVERED  Final Report for Period 22 May 1978—1 June 1978
7. AUTHOR(s)  K. Triebes		6. PERFORMING ORG. REPORT NUMBER PIFR-1050-2
9. PERFORMING ORGANIZATION NAME AND ADDRESS  Physics International Company 2700 Merced Street San Leandro, California 94577		8. CONTRACT OR GRANT NUMBER(s)  DNA 001-77-C-0193
11. CONTROLLING OFFICE NAME AND ADDRESS  Director Defense Nuclear Agency Washington, D.C. 20305		10. PROGRAM ELEMENT, PROJECT, TASK AREA & WORK UNIT NUMBERS  NWED Subtask N99QAXAK112-07
14. MONITORING AGENCY NAME & ADDRESS(if different from Controlling Office)		12. REPORT DATE  September 1978
		13. NUMBER OF PAGES 54
		15. SECURITY CLASS (of this report)  UNCLASSIFIED
		15a. DECLASSIFICATION/DOWNGRADING SCHEDULE
16. DISTRIBUTION STATEMENT (of this Report)  Approved for public release; distribution unlimited.		
17. DISTRIBUTION STATEMENT (of the abstract entered in Block 20, if different from Report)		
18. SUPPLEMENTARY NOTES  This work sponsored by the Defense Nuclear Agency under RDT&E RMSS Code B342077464 N99QAXAK11207 H2590D.		
19. KEY WORDS (Continue on reverse side if necessary and identify by block number)  Carbon Phenolic Electron Beam Magnetic Field Ablator Heat Shield  ② 39 cm		
20. ABSTRACT (Continue on reverse side if necessary and identify by block number)  The OWL II generator, in conjunction with the large area beam hardware, generated a reproducible uniform electron beam capable of removing between 0.013 and 0.025 cm depth of phenolic from carbon phenolic ablator surfaces. The beam had a diameter of 19 cm (280 cm <sup>2</sup> ). Specimens of staple rayon and continuous filament rayon carbon phenolic were irradiated. Samples included both flat and conical section configurations. Stress pulse measurements were performed on each type of material using quartz gages. The irradiated		

UNCLASSIFIED

SECURITY CLASSIFICATION OF THIS PAGE(When Data Entered)

20. ABSTRACT (Continued)

specimens were forwarded to Science Applications Inc., and Prototype Development Associates for further testing.

A

UNCLASSIFIED

SECURITY CLASSIFICATION OF THIS PAGE(When Data Entered)

## CONTENTS

	<u>Page</u>	
SECTION 1	INTRODUCTION	3
SECTION 2	DESCRIPTION OF THE EXPERIMENT	4
SECTION 3	EXPERIMENTAL DATA	15
SECTION 4	CONCLUSIONS AND RECOMMENDATIONS	25
REFERENCES		26
APPENDIX	CALCULATED DEPTH DOSE PROFILES	A-1

Accession For	
NTIS GMA&I	<input checked="" type="checkbox"/>
DDC TAB	<input type="checkbox"/>
Unannounced	<input type="checkbox"/>
Justification	<input type="checkbox"/>
By _____	
Distribution/ _____	
Availability Codes	
Dist	Avail and/or special
A	

## ILLUSTRATIONS

<u>Figure</u>		<u>Page</u>
1	Schematic of Ablator Experiment	5
2	Pulse Charge Voltage Versus Anode/Cathode Gap for Various Diode Voltages	7
3	Fluence Versus Anode/Cathode Gap for 410-cm <sup>2</sup> Diode on OWL II	8
4	Effect of Filter on Electron Beam as a Function of Voltage	9
5	Representative Energy Deposition Profile	10
6	Quartz Gage Geometry	12
7	Frustrum Mounting Hardware	13
8	Top Section View of Masking Technique Showing e-Beam Orientation with Respect to Frustrum Sample	14
9	Beam Exposure Pattern for Frusta	17
10	Individual Frusta	18
11	Assembled Cone	19
12	Quartz Gage Data	21
13	Quartz Gage Data	22
14	Quartz Gage Data	23

## SECTION 1

### INTRODUCTION

This report describes experimental work performed under contract DNA 001-77-C-0193 between May 22, 1978, and June 1, 1978, on the Defense Nuclear Agency OWL II large-area beam facility. The objective of this effort was to obtain samples of staple rayon (SR) and continuous filament rayon (CFR) carbon phenolic ablator materials with the phenolic removed to a uniform depth of between 0.013 cm and 0.025 cm by irradiating specimens with a large-area pulsed electron beam. Both flat and conical section samples were successfully irradiated and then sent on to Science Applications Inc. (SAI) and Prototype Development Associates (PDA) for further testing. On selected SR and CFR flat samples the stress-time histories at the rear surfaces of the 1.27-cm-thick specimens were monitored with  $1.1-\mu\text{s}$  quartz gages. The average diode mean voltage for this test series was 320 kV with an average fluence of  $17 \text{ cal/cm}^2$ . After filtering and magnetic compression the electron beam at the target location had an effective mean energy of 270 kV, a fluence of  $10 \text{ cal/cm}^2$ , and an estimated mean angle of incidence of 57 degrees. The area of irradiation at the target was  $280 \text{ cm}^2$ . This constitutes a 50 percent increase in beam area for these phenolic removal conditions over what was achieved in the previous experimental series (Reference 1).

## SECTION 2

### DESCRIPTION OF THE EXPERIMENT

A schematic of the large-area beam system with axial magnetic transport used in this experiment is shown in Figure 1. This is the same hardware as was used in the experiment reported previously under this contract. Prior to this testing, however, an analytical parameter study was carried out for the OWL II machine in an effort to maximize the available beam area within the context of the existent hardware. This was deemed necessary since some of the conical section samples (frusta) would fit within the area of the previous beam with little margin for error. By maximizing the beam area the sample alignment constraints were relaxed, allowing faster shot-to-shot turn-around times during the experiment.

With an experiment of this type the two prime variables are the pulse charge voltage and the anode-cathode separation. The pulse charge voltage is the voltage at which the main switch in the generator closes. The diode voltage  $V_D$  is related to the pulse charge,  $V_{pc}$ , by the following equation:

$$V_D = \frac{0.68 V_{pc} Z_L}{1.9 + Z_L}$$

and  $Z_L$  is the diode impedance. Figure 2 illustrates the calculated relationship between pulse charge and anode cathode spacing for a range of diode voltages. The OWL II generator is designed to deliver a 1-MeV, 0.55-kA pulse into a 1.9-ohm diode matched load.

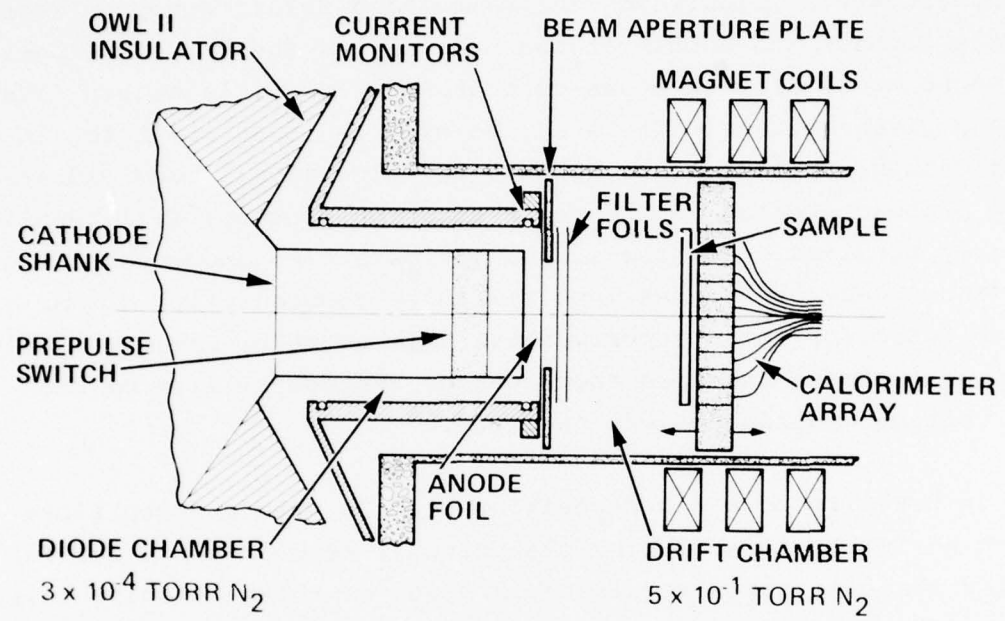


Figure 1 Schematic of ablator equipment.

At this voltage, however, the phenolic would be removed to a far greater depth than desired; the object of the parameter study was to determine the lowest voltage that could be achieved while still obtaining sufficient fluence to remove the phenolic to the required depth. Figure 3 illustrates the calculated relationship between average fluence and anode-cathode spacing for the 410- $\text{cm}^2$  diode. As can be seen, smaller anode-cathode spacings yield higher fluences for any given voltage. There is, however, a lower limit for the anode cathode spacing since below a certain value, diode closure (from plasmas created in the field emission process) will result in early termination of the pulse. Below a 6-mm anode-cathode gap the diode behavior becomes less reliable; consequently, a 7-mm gap was selected for these experiments. This geometry yielded stable diode performance and good shot-to-shot reproducibility of both mean voltage and fluence was obtained.

In order to obtain a deposition profile with a steep slope (which maximizes control over the phenolic removal depth for the shallow removal depths required), a 0.005-cm-thick titanium filter was positioned between the diode and the sample. The effect of this filter is to reduce the kinetic energy of the electrons, increase their mean angle of incidence, and reduce the beam fluence. Figure 4 illustrates the effect of the filter on the energy and estimated angle of incidence of the beam as a function of mean diode voltage. For the average shot conditions for this series, the 320-kV diode voltage is reduced by 50 kV in passing through the filter and the emerging e-beam is estimated to have an average angle of incidence of 57 degrees. An example of the deposition profile from a typical shot, 4375, is shown in Figure 5. On this pulse the mean voltage was 316 kV, the fluence was 17.6 cal/ $\text{cm}^2$ , and the depth of removal was measured at 0.015 cm. The first part of the profile (shaded portion) is the deposition in the titanium anode and filter, which have a total thickness of

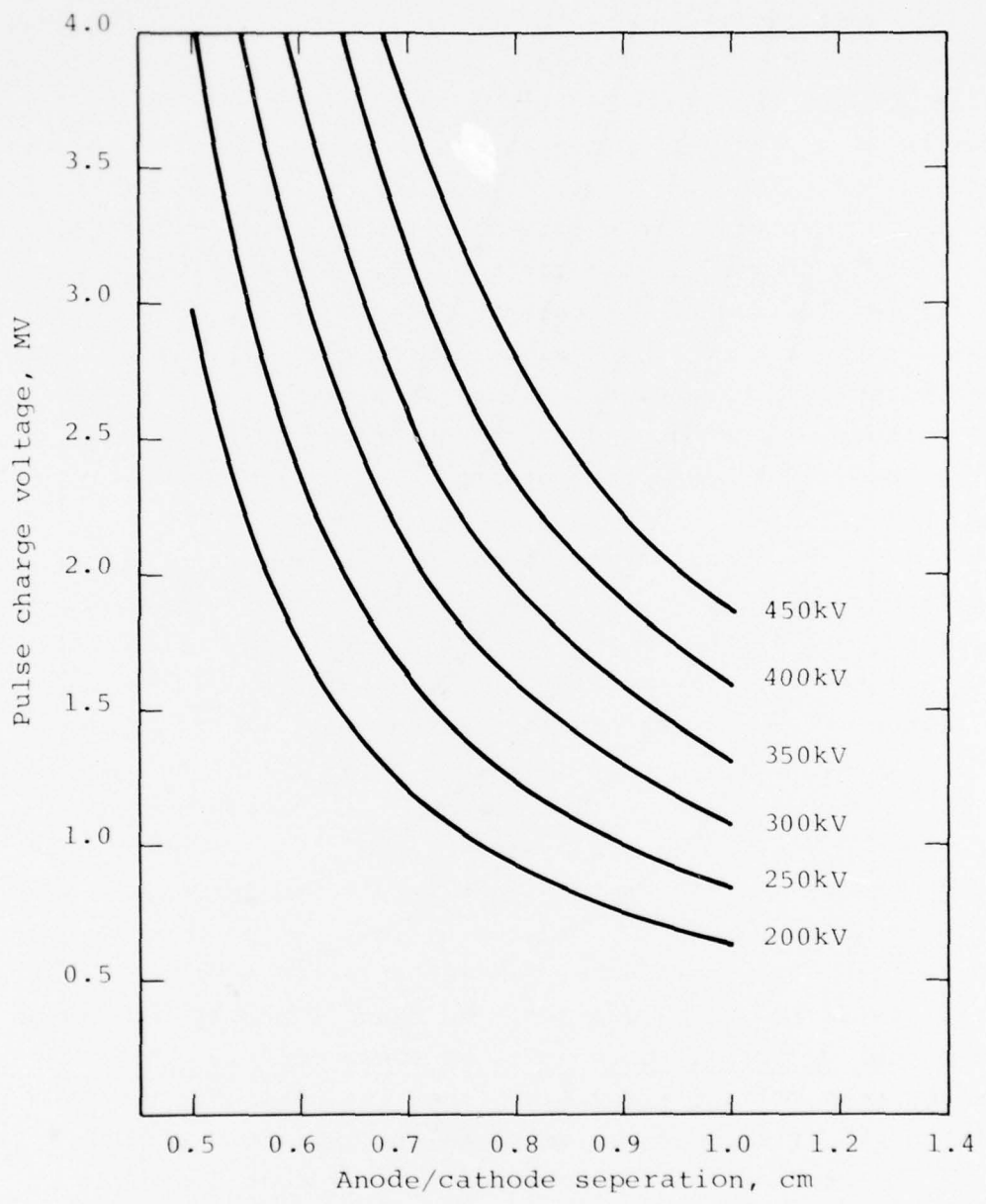


Figure 2 Pulse charge voltage versus anode/cathode gap for various diode voltages.

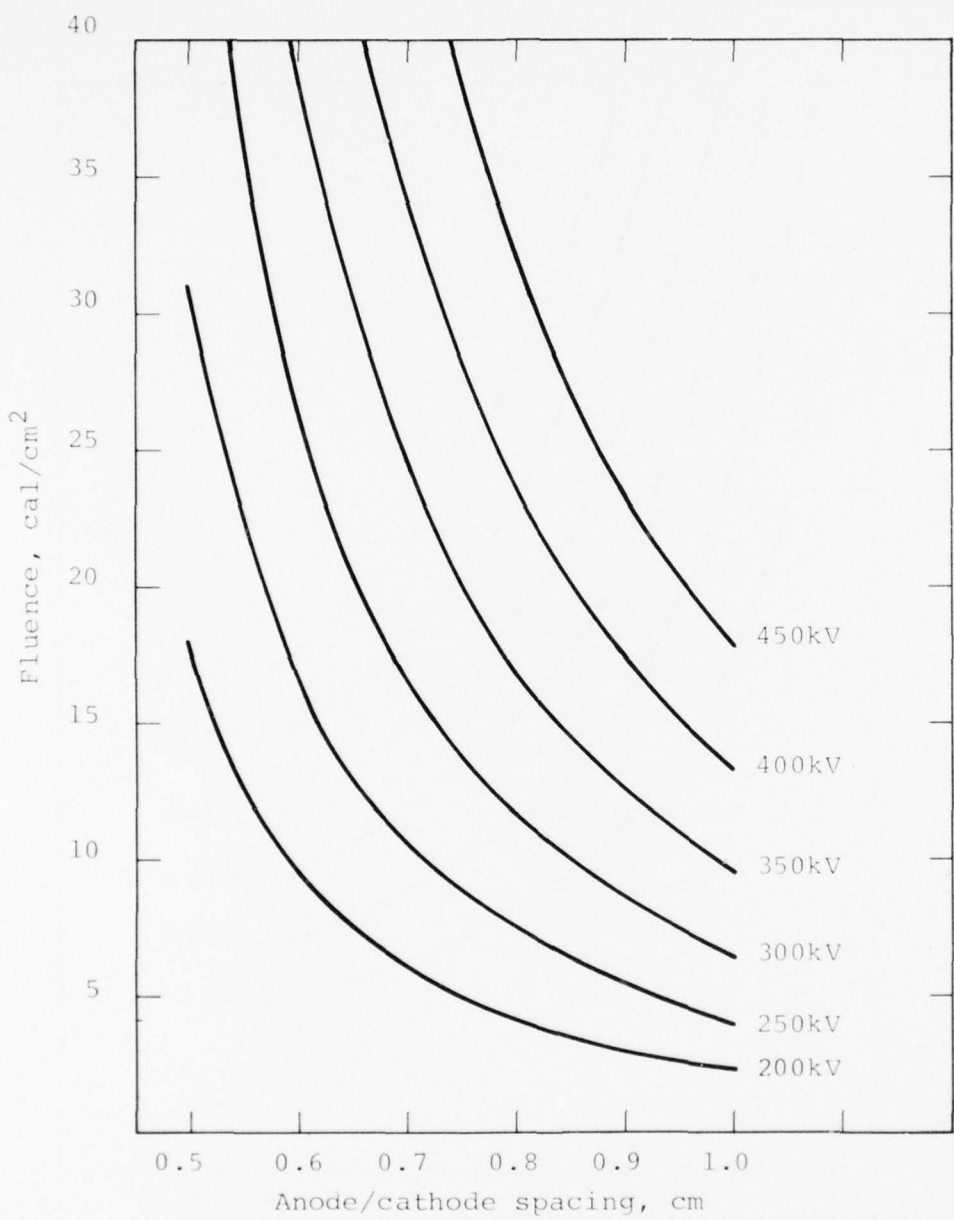


Figure 3 Fluence versus anode/cathode gap for 410-cm<sup>2</sup> diode on OWL II.

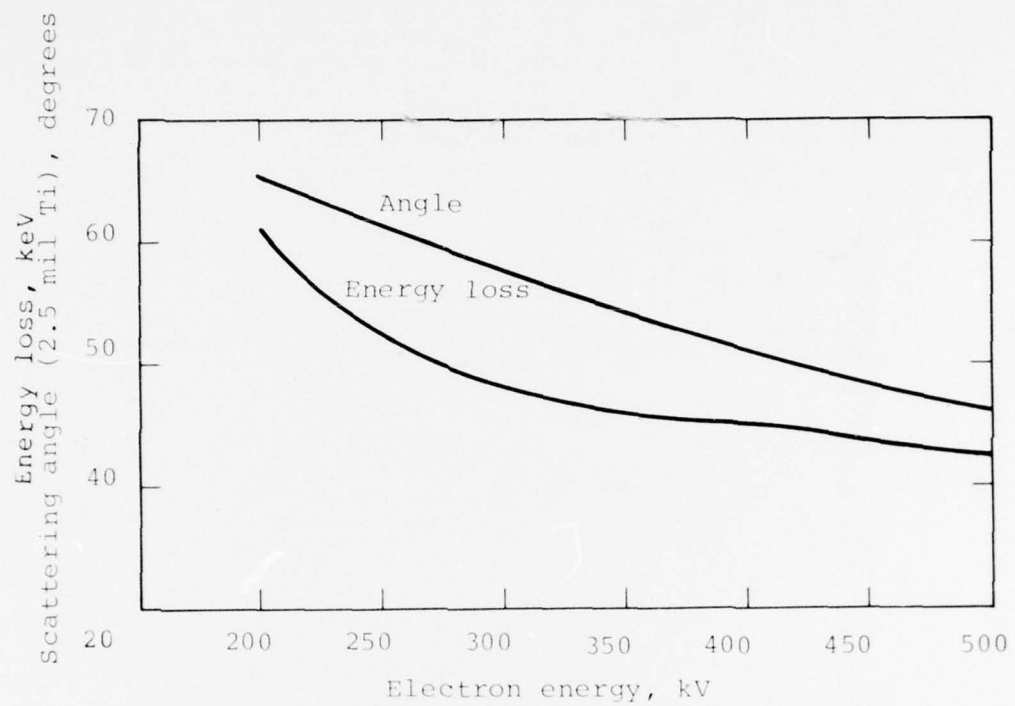


Figure 4 Effect of filter on electron beam as a function of voltage.

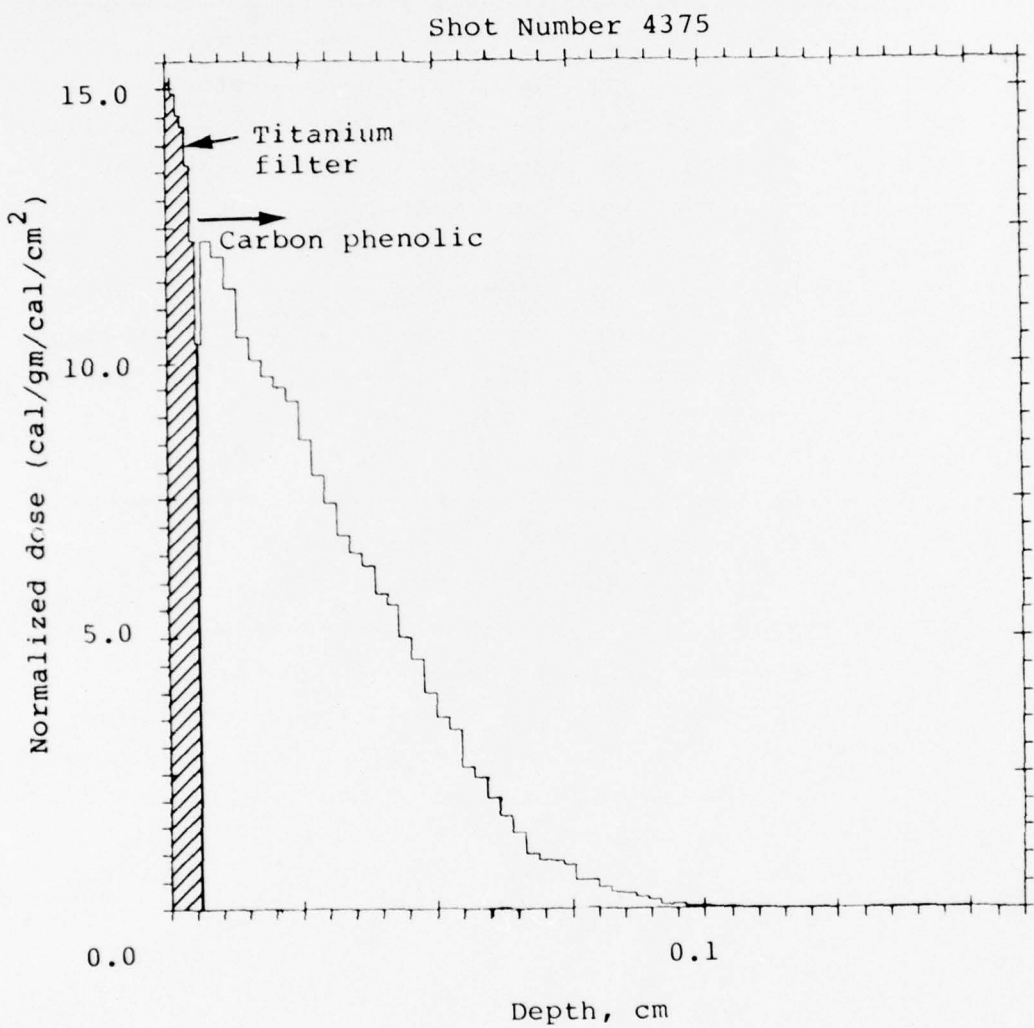


Figure 5 Representative energy deposition profile.

0.0064 cm. At the removal depth of 0.015 cm the normalized dose is 9.5 cal/gm per cal/cm<sup>2</sup>, which combined with the measured diode fluence of 17.6 cal/cm<sup>2</sup> and beam compression by a factor of 1.2 indicates a dose of 201 cal/gm at the depth within the sample. This value corresponds to the generally accepted threshold value for phenolic removal of 200 cal/gm. Calculated depth dose profiles for all sample shots are presented in the appendix of this report. These profiles are calculated directly from the voltage and current waveforms obtained on the individual shots.

All flat samples irradiated during this test series were mounted in a graphite mask and backed with 0.635-cm-thick plexiglass to prevent rear surface spall. The original experimental plan was to have the flat samples unbacked unless severe rear surface spall was observed. Pulse 4372 showed a great amount of rear surface spall; all subsequent flat samples, therefore, had plexiglass backers coupled with vacuum grease.

Samples intended for stress-time measurements were lapped flat on their rear surface before bonding the quartz gages. Backers for these samples had a hole cut in the center to accommodate the gages. A schematic of the mounting scheme is shown in Figure 6. Furane 202 epoxy was used to bond the quartz gages to the samples with bond thickness of  $\leq 1.2 \times 10^{-3}$  cm. All quartz gages had an outside diameter of 3.175 cm, a guard ring diameter of 1.270 cm and a thickness of 0.635 cm, which provides a readtime of 1.1  $\mu$ s.

Frusta or conical section samples were mounted on a special fixture fabricated by PDA. Front and side views of this mounting hardware are shown in Figure 7. Because of the relative sizes of the frusta and the beam irradiation area, two shots were required to fully irradiate each section. The unirradiated portion was

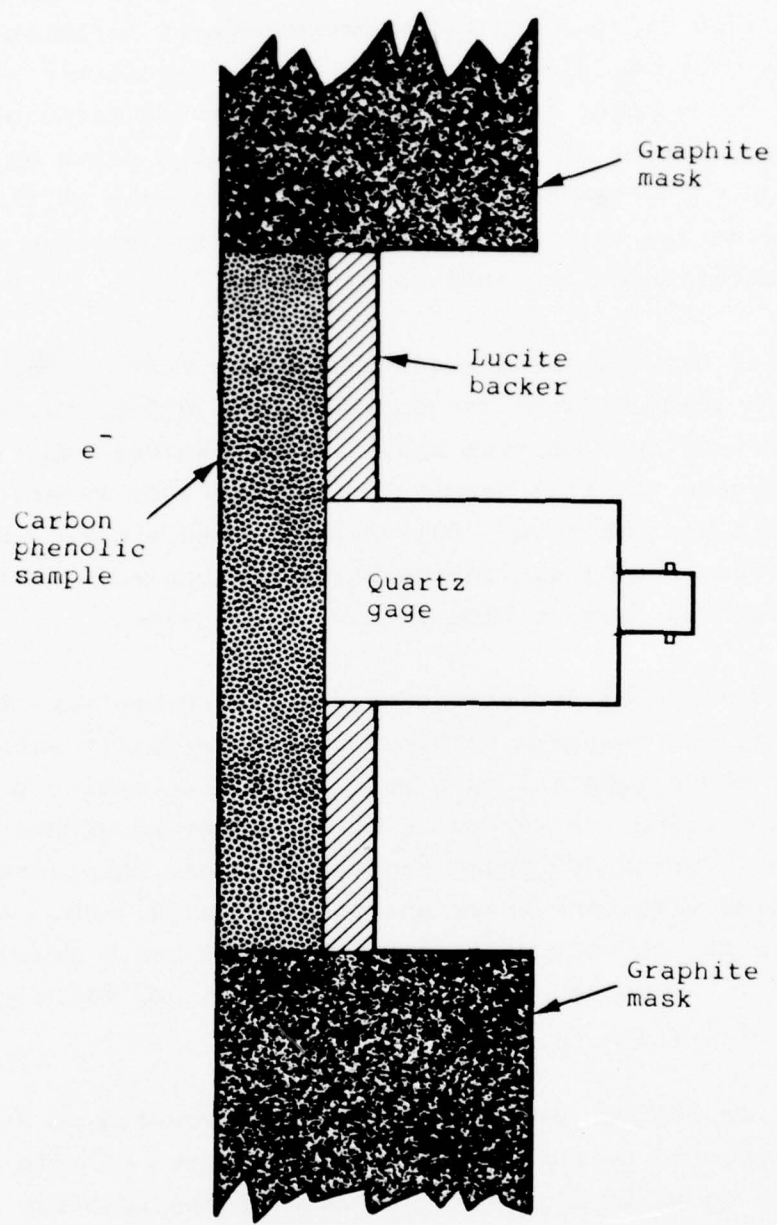


Figure 6 Quartz gage geometry.

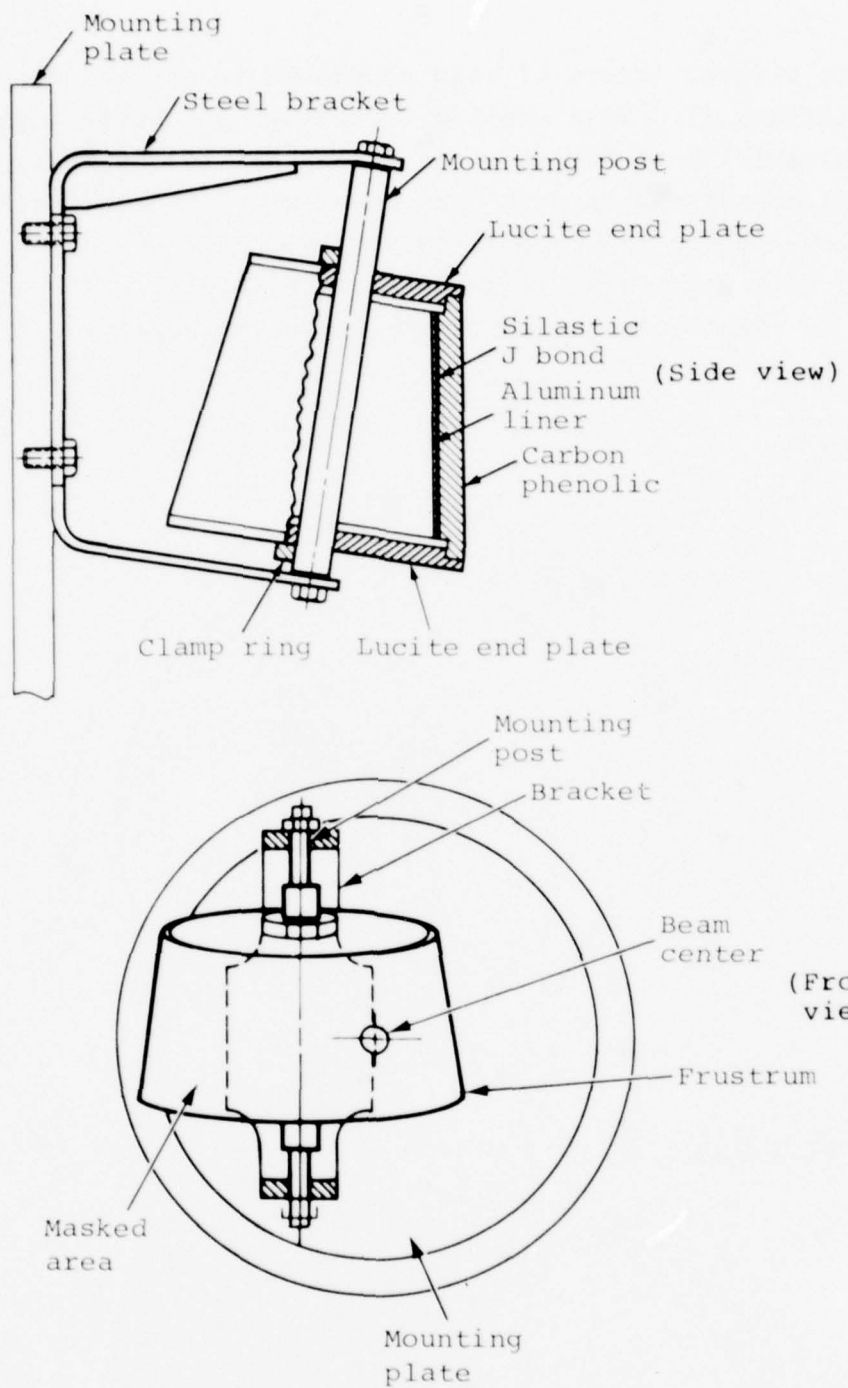


Figure 7 Frustum mounting hardware.

masked with several layers of thin cardboard to prevent double exposure (Figure 8). This masking technique was chosen because of its adaptability to curved surfaces and was tested during the first experimental series with good results. Although the flat samples were all located at a 10-cm distance from the anode plane, the frusta were positioned with their closest point at 7.5 cm from the anode to compensate for the depth of these samples.

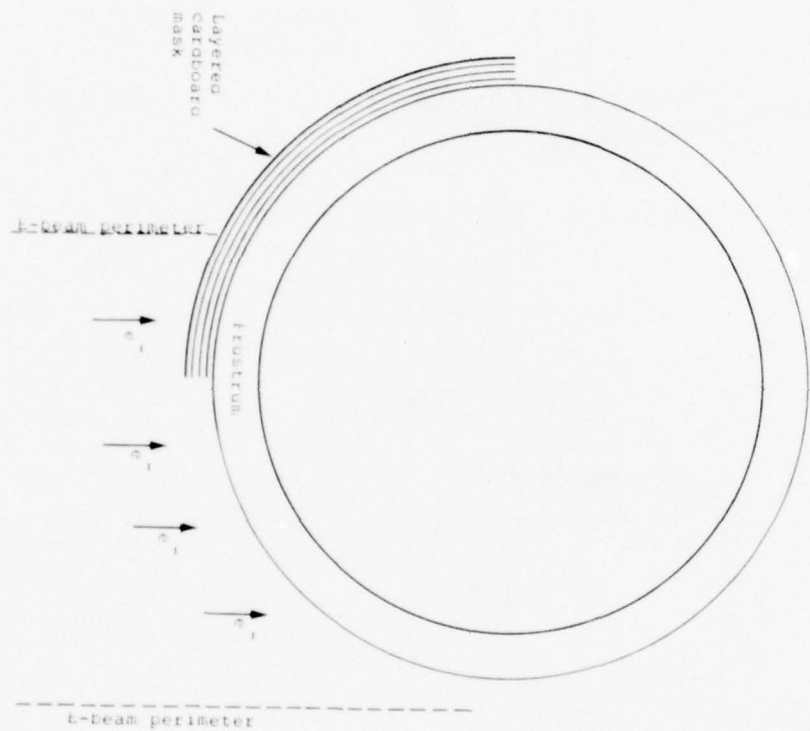


Figure 8 Top section view of masking technique showing e-beam orientation with respect to frustum sample.

## SECTION 3

### EXPERIMENTAL DATA

A summary of all data recorded during this experiment is listed in Table 1. As noted in Section 2, the average beam conditions were 320-kV mean diode voltage and  $17 \text{ cal/cm}^2$  fluence; the average removal depth was 0.015 cm and average mass loss,  $43 \text{ mg/cm}^2$ . On all fluence and sample shots a 1-cm<sup>2</sup> area control sample block of CP was exposed near the edge of the beam. The weight of the sample block was recorded before and after the shot in order to monitor the mass loss per unit area. Phenolic removal depth was measured on the main sample with a knife-edge vernier caliper for all flat specimens. On fluence and frusta shots the phenolic removal depth was measured on the 1-cm<sup>2</sup> control samples.

For the frusta samples the average diode fluence was  $18 \text{ cal/cm}^2$  with an average mean voltage of 320 kV. A summary of the frusta data is shown in Figure 9. Two sectioned conical samples of CP were available for testing. In one case the cone had an aluminum liner bonded with a 0.1 cm thick Sylastic J bond. The other cone had no liner. All frusta from the lined cone were exposed to the electron beam. On frustum sample 955412-3, however, both exposures were low fluence ( $12.3 \text{ cal/cm}^2$  average) and the beam appeared somewhat uneven. These shots were repeated with the corresponding section of the unlined cone. No other frusta from the unlined cone were tested. Photos of all irradiated frusta are shown in Figure 10 and the assembled cone is shown in Figure 11.

TABLE 1  
DATA SUMMARY

Shot	Shot Type	Anode-Cathode Spacing (cm)	Anode-Target Spacing (cm)	Pulse Charge Voltage (MV)	Diode Voltage (KV)	Diode Fluence (cal/cm <sup>2</sup> )	Phenolic Removal Depth (cm)	Control Sample Mass Loss (mg)	Peak Stress (Kbar)	Sample I.D.
4361	Short	0	--	--	1.82	--	--	--	--	--
4362	Short	0	--	--	1.82	--	--	--	--	--
4363	Short	0	--	--	1.82	--	--	--	--	--
4364	Fluence	0.7	10	2.28	310	16.0	0.013	--	--	--
4365	Fluence	0.7	10	2.37	300	15.6	0.010	4.2	--	--
4366	Witness plate	0.3 cm poly	0.7	10	2.37	308	16.0	0.015	5.9	--
4367	Quartz gage SR	0.7	10	2.46	345	18.6	0.023	--	2.34	K
4368	5x7.5 cm <sup>2</sup> sample	0.7	10	2.00	270	11.7	0.003	--	--	J, F
4369	1 SR + 1 CFR samples	0.7	10	2.20	270	11.7	0.003	--	--	--
4370	Fluence	0.7	10	2.50	348	20.1	0.016	6.7	--	--
4371	Fluence	0.7	10	2.64	345	19.3	0.013	6.9	--	--
4372	Quartz gage	10 cm SR	0.7	10	3.20	325	19.1	0.023	--	5.02
4373	Unbaked 2 samples	0.7	10	2.92	322	16.6	0.015-0.020	5.3	--	57/38
4374	Quartz gage CFR	0.7	10	2.92	324	17.0	0.015	5.3	3.77	6
4375	10x10 cm <sup>2</sup> , backed	0.7	10	2.92	320	17.6	0.015-0.020	3.8	--	E37
4376	5x7.5 cm <sup>2</sup> , samples	0.7	10	2.92	330	18.6	0.015	3.9	--	955412-4
4377	Base frusta	0.7	7.5	2.92	265	14.0	0.018	4.5	--	--
4378	1st exp., fluence	0.7	7.5	2.92	315	16.3	0.008	2.6	--	955412-4
4379	Base frusta, 2nd exp.	0.7	7.5	2.92	315	16.3	0.008	2.6	--	--
4380	Quartz gage SR, backed	0.7	10.0	2.92	308	15.9	0.018	5.3	4.20	16
4381	Frusta, 1st exp.	0.7	7.5	2.92	307	13.7	--	--	--	955412-3
4382	Quartz gage CFR	0.7	10.0	2.92	275	14.3	0.020	--	3.16	5
4383	10x10 cm <sup>2</sup> , backed	0.7	10.0	2.92	253	10.8	0.005	1.3	--	955412-3
4384	Frusta, 2nd exp.	0.7	7.5	2.92	329	17.4	0.028	7.9	--	--
4385	Frusta, 1st exp.	0.7	7.5	2.92	342	21.3	0.018	3.7	A	955412-2
4386	Frusta, 2nd exp.	0.7	7.5	2.92	304	16.1	0.013	2.5	--	955412-2
4387	Tip frusta	0.7	7.5	2.92	370	19.9	0.010	3.1	--	955412-2
4388	1st exp.	0.7	7.5	2.92	316	16.8	--	--	--	955412-1
4389	Fluence	0.7	10.0	--	352	18.3	0.025	7.3	--	955412-1
4390	Tip frusta	0.7	7.5	2.55	365	18.1	--	--	--	C
4391	Quartz gage SR	0.7	10.0	2.55	317	19.5	0.036	4.4	2.57	--
4392	10x10 cm <sup>2</sup> , backed	0.7	10.0	2.55	Machine Malfunction	0.033	1.57	--	--	--
4393	Frusta, unbaked	0.7	10.0	1.74	349	21.0	0.033	--	--	--
4394	Frusta, unbaked	0.7	10.0	2.73	Machine Malfunction	0.033	1.57	--	--	--
4395	1st exp.	0.7	7.5	2.55	300	18.1	0.023	--	--	56
4396	5x7.5 sample SR	0.7	10.0	2.55	331	19.0	0.023	--	--	--
4397	Frusta, unbaked	0.7	7.5	2.56	307	19.1	--	--	--	--
4398	2nd exp.	0.7	10.0	2.71	318	16.9	0.015	4.3	--	--
Series Average		0.7	--	--	--	--	--	--	--	--

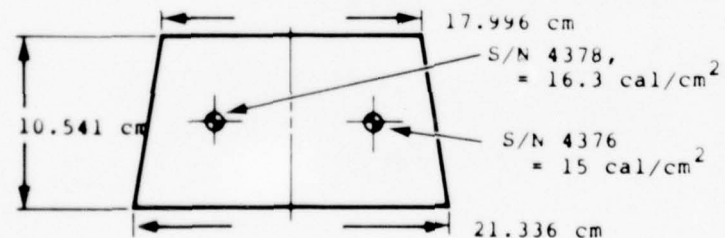
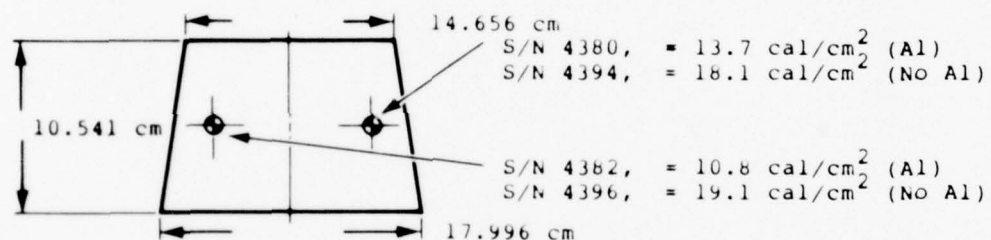
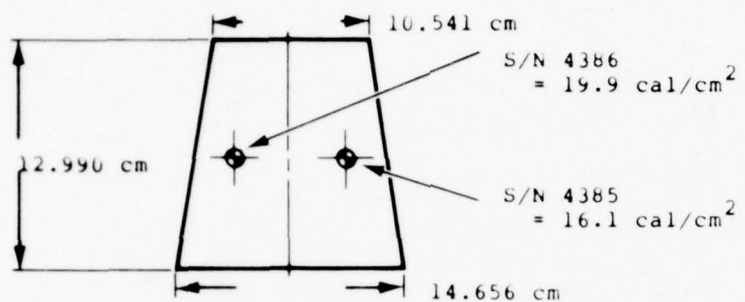
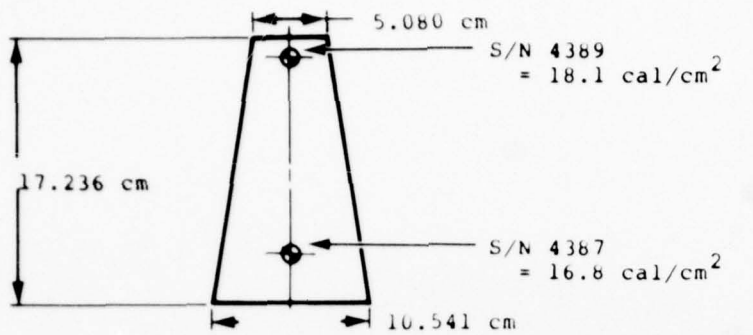


Figure 9 Beam exposure pattern for frustra.

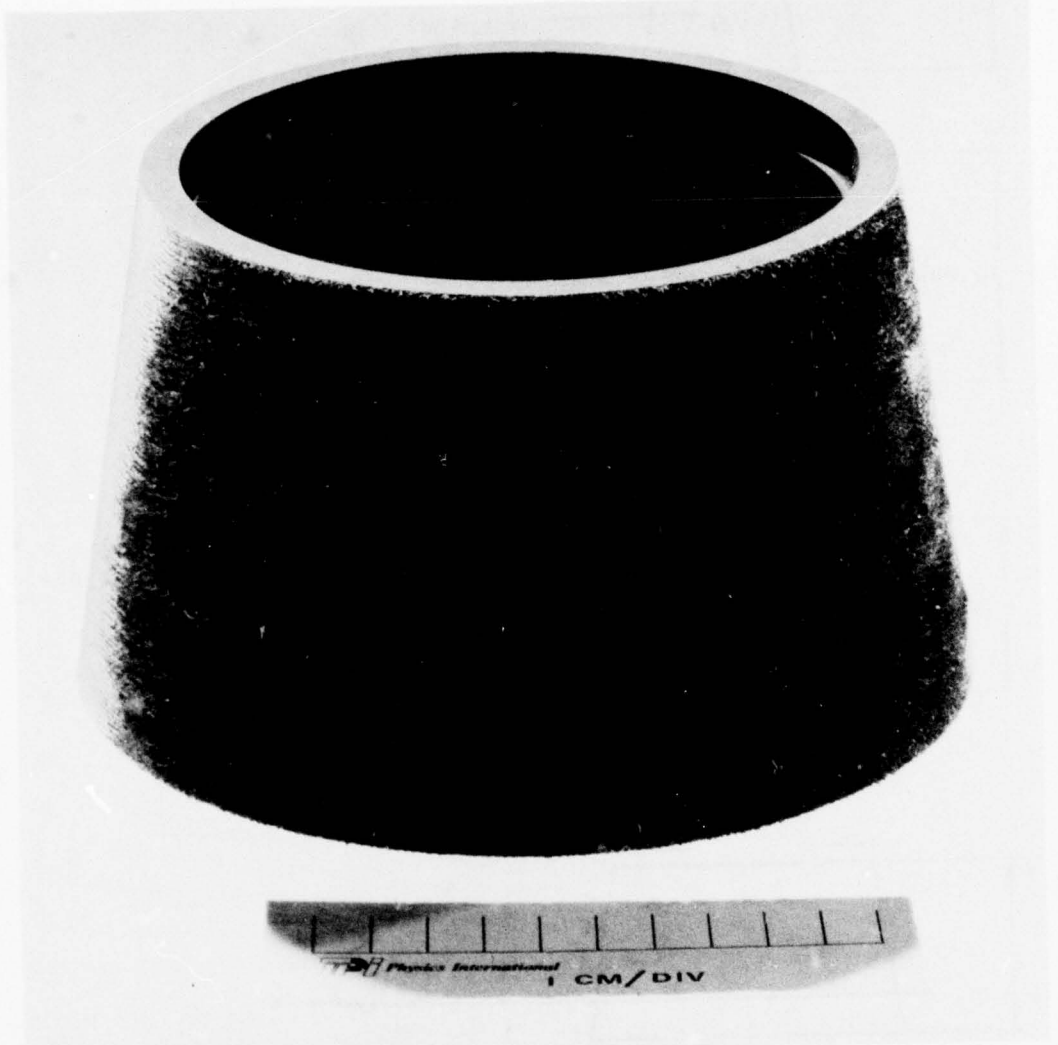


Figure 10 Individual frusta.

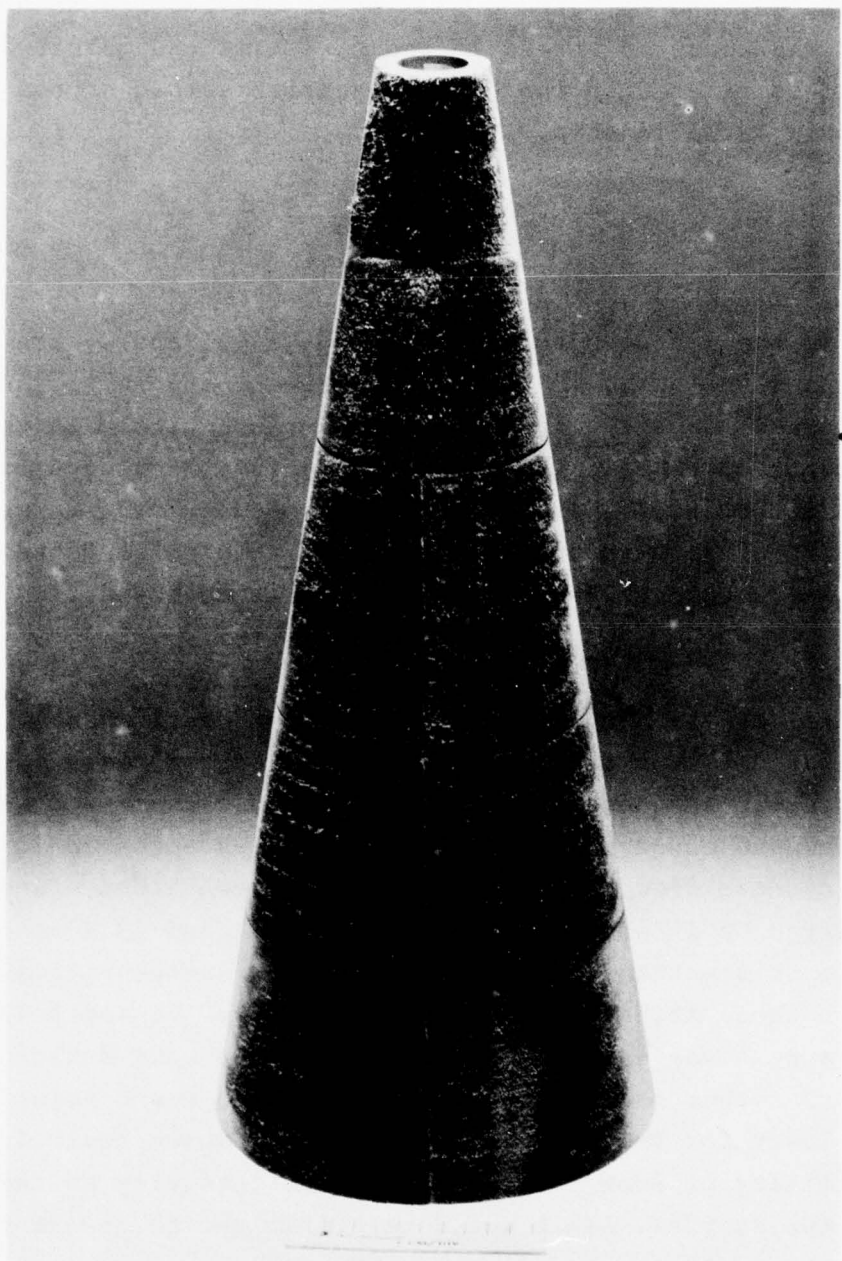


Figure 11 Assembled Cone.

The raw quartz gage data from this test are shown in Figures 12, 13, and 14, with a summary of the reduced data in Table 2. The measured stress is the stress in the quartz gage itself and is related to the carbon phenolic sample stress by the following relationship,

$$\sigma_s = \sigma_g \frac{p_s c_s + \rho_g c_g}{2 \rho_g c_g}$$

where  $\sigma_g$  is the measured stress in the gage,  $\rho_g$  and  $c_g$  are the density and sound speed in the gage material, and  $\sigma_s$ ,  $p_s$  and  $c_s$  are the stress, density, and sound speed respectively in the carbon phenolic sample. The gage is made from x-cut quartz and has a density of  $2.65 \text{ g/cm}^3$  and a sound speed of  $5.73 \text{ mm}/\mu\text{s}$ . For the carbon phenolic the density was  $1.45 \text{ g/cm}^3$  and the sound speed varied between  $3.40$  and  $3.87 \text{ cc}/\mu\text{s}$ , as measured from the gage records.

A total of six samples were tested with quartz gages, two CFR and four SR. For the CFR samples, the stress measurements were consistent and the relationship between fluence and peak stress appeared constant. The four SR samples appeared to be divided into two groups where the ratio between fluence and peak stress varied by a factor of two. Shots 4372 and 4379 were mutually consistent and exhibited stress-to-fluence ratios similar to those observed for the CFR samples. On shots 4367 and 4390 the stress was well below what would have been anticipated based on the other measurements. The observed sound velocity was also lower for those shots ( $3.40 \text{ mm}/\mu\text{s}$ ), which could indicate the possibility of some reduced mechanical integrity on the part of these two samples. This would be sufficient to reduce the measured stress to the levels observed.

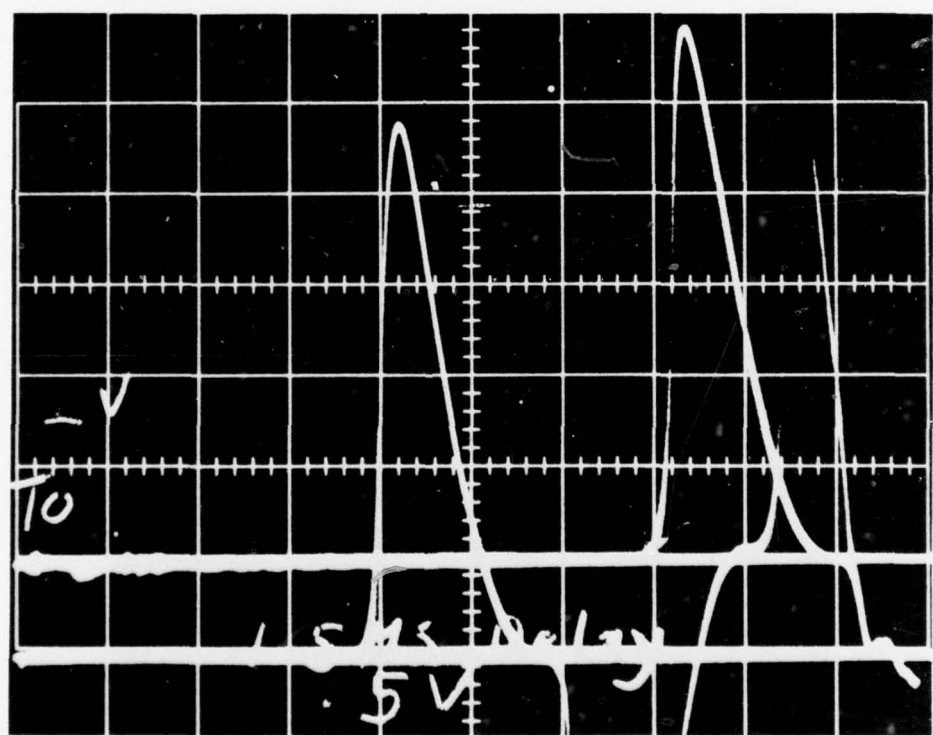
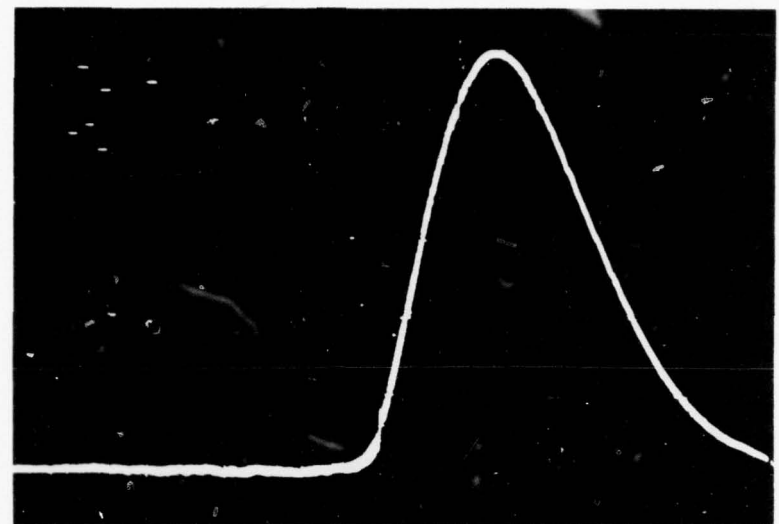


Figure 12 Quartz gage data (shots 4367 and 4372).

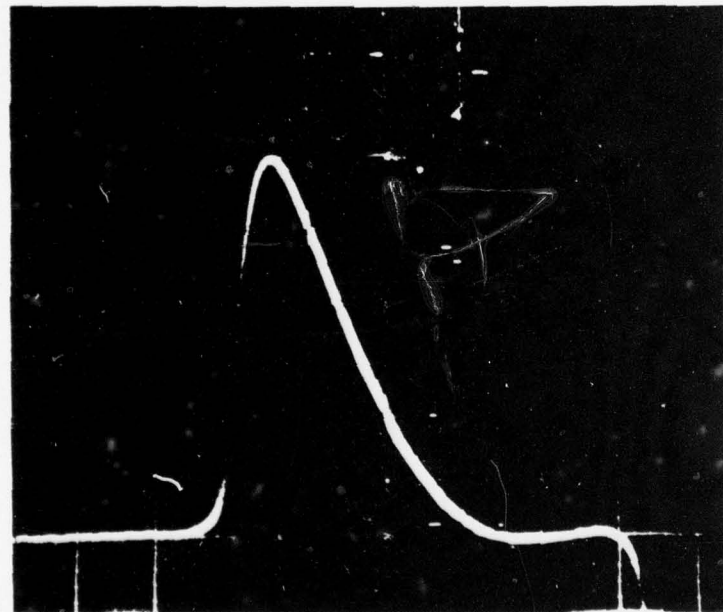
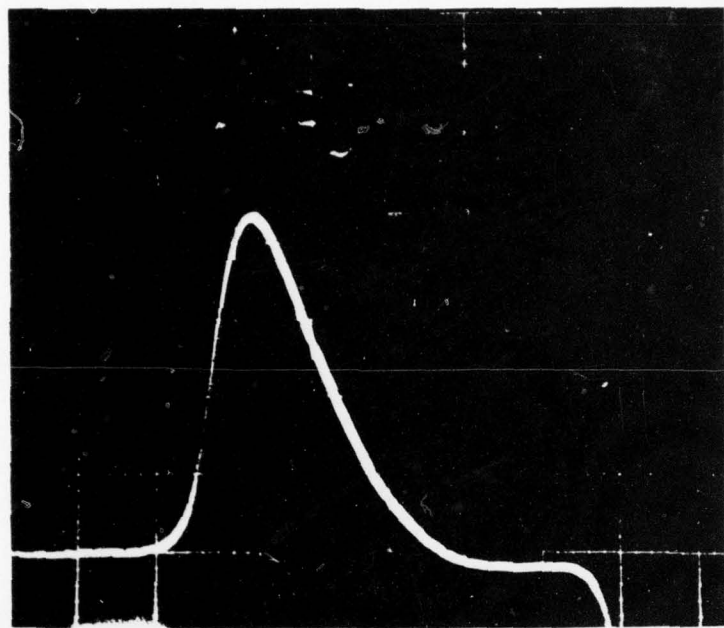


Figure 13 Quartz gage data (shots 4374 and 4379).

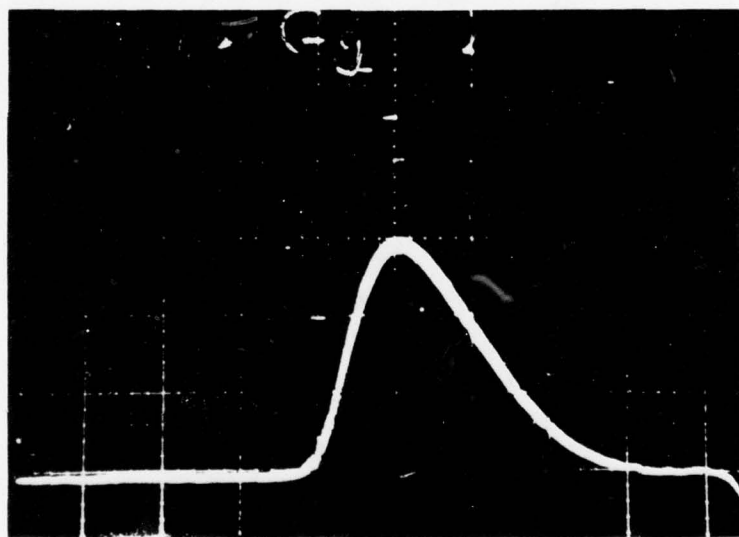
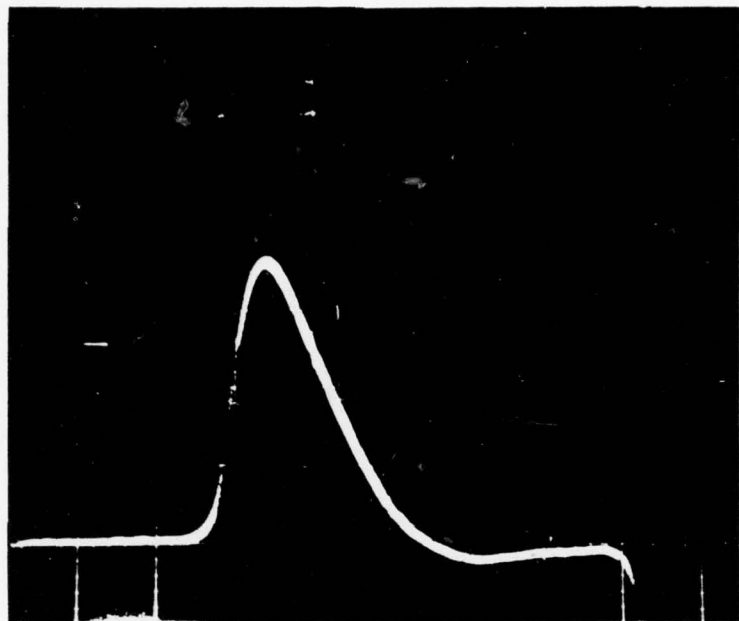


Figure 14 Quartz gage data (shots 4381 and 4390).

TABLE 2  
QUARTZ GAGE DATA

Shot	Diode Voltage (kV)	Mean Diode Fluence (cal/cm <sup>2</sup> )	Diode Gage	Peak Stress (kbar)	Sample	Pulse Width (ns)	Pulse Velocity mm/ $\mu$ s	Sample Type	Sample I.D.
4367	345	18.6	2.34	1.55	496	3.40	SR	K	
4372	330	19.1	4.93	3.35	364	3.76	SR	15	
4374	323	17.0	3.77	2.58	310	3.87	CFR	6	
4379	312	15.9	4.20	2.85	304	3.75	SR	16	
4381	279	14.3	3.16	2.14	264	3.74	CFR	5	
4390	335	19.5	2.57	1.71	405	3.46	SR	C	

## SECTION 4

### CONCLUSIONS AND RECOMMENDATIONS

The OWL II generator, in conjunction with the large-area beam hardware, generated a reproducible uniform electron beam capable of removing between 0.013 and 0.025 cm depth of phenolic from carbon phenolic ablator surfaces. The beam had a diameter of 19 cm ( $280 \text{ cm}^2$ ), which constitutes a 40-percent improvement in beam area over that used to obtain the same removal conditions during the previous experiment. Any further substantial increase in area would require a major redesign of the diode hardware. With new hardware it is possible that a factor of almost four increase in beam area may be possible on the OWL II' configuration on the generator.

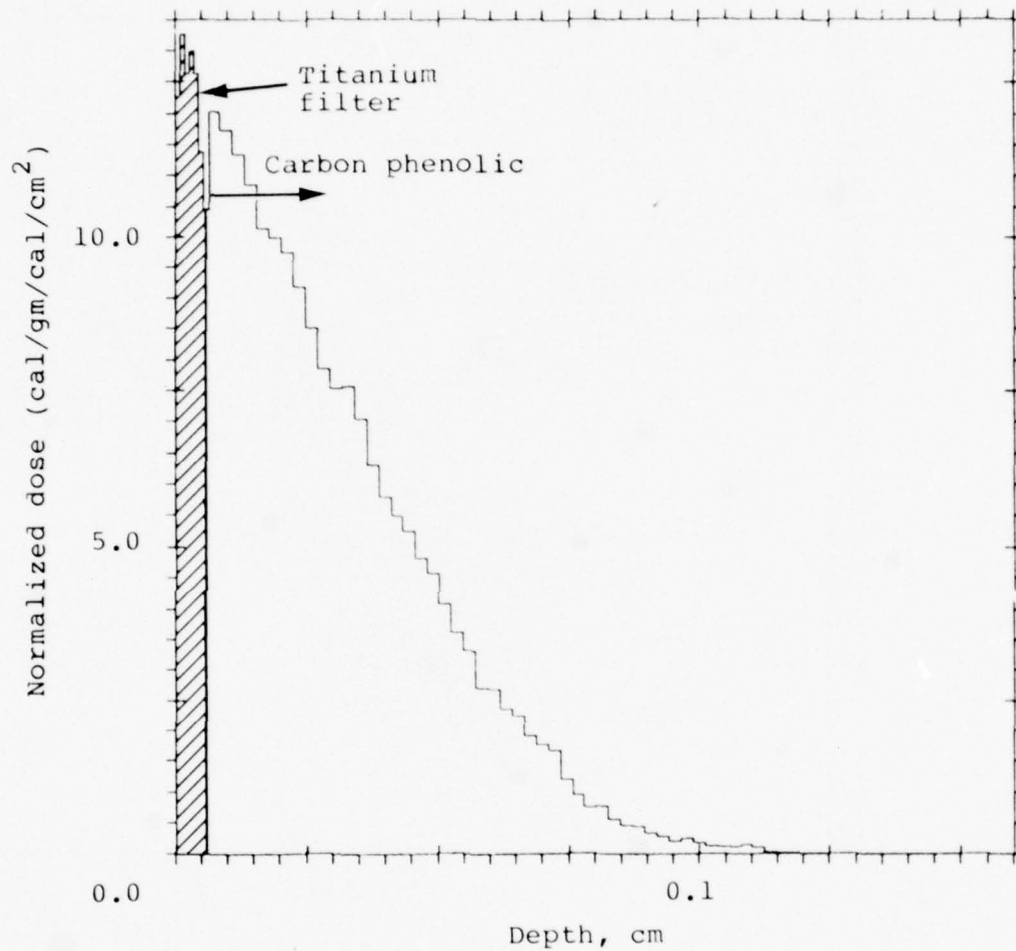
A second area of possible improvement is related to the masking of samples when multiple beam exposures are planned on a single specimen. On all frusta exposed during this series a narrow ridge of phenolic remains between the two beam exposures in spite of efforts to eliminate this through repositioning of the mask. Subsequent tests by PDA will determine whether these ridges present a problem in ablation or aerodynamic experiments. If the ridge effect is significant, some experimental effort should be dedicated to developing a more efficient mask prior to further sample irradiation.

## REFERENCES

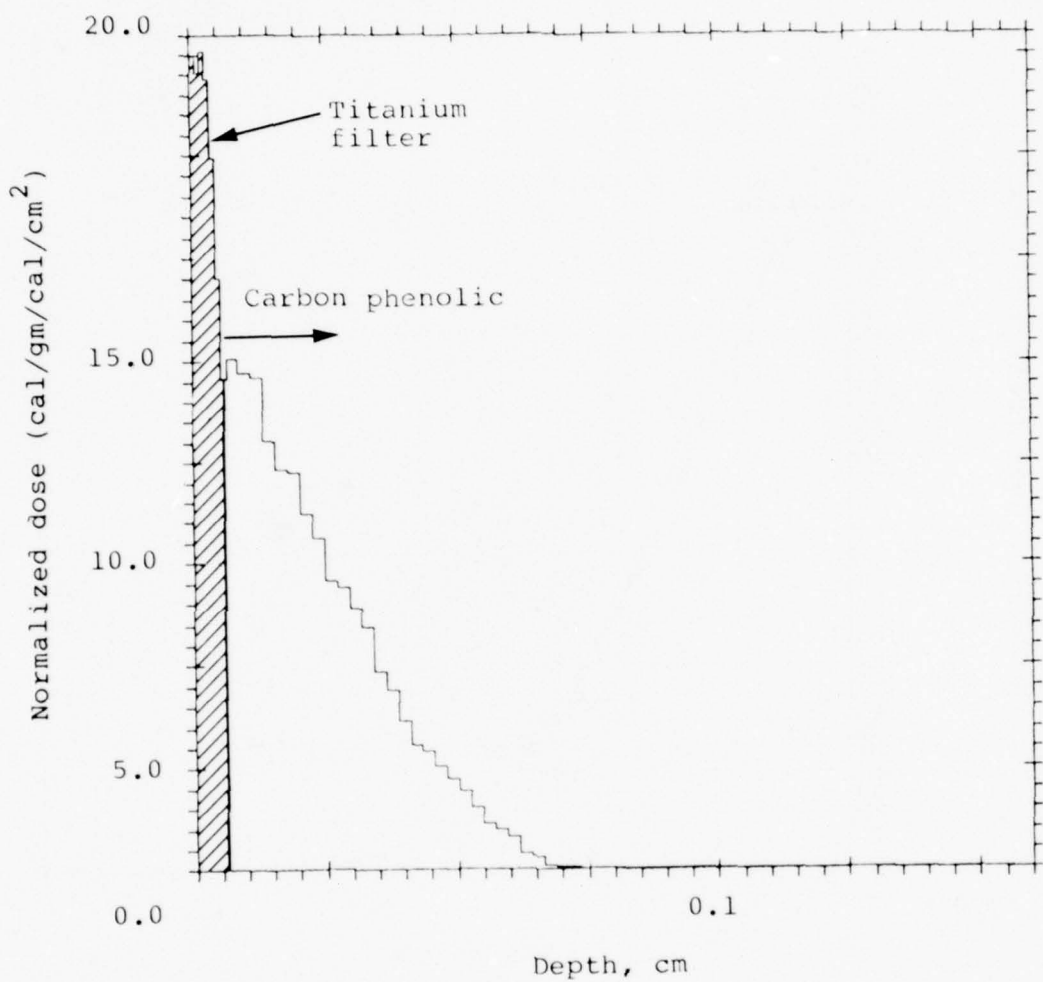
1. K. Triebes, C. Stallings, and J. Shea, Electron Beam Conditioning of Carbon Phenolic Ablator Surface, DNA 4522F, June 1978.

APPENDIX  
CALCULATED DEPTH DOSE PROFILES

Shot Number 4367

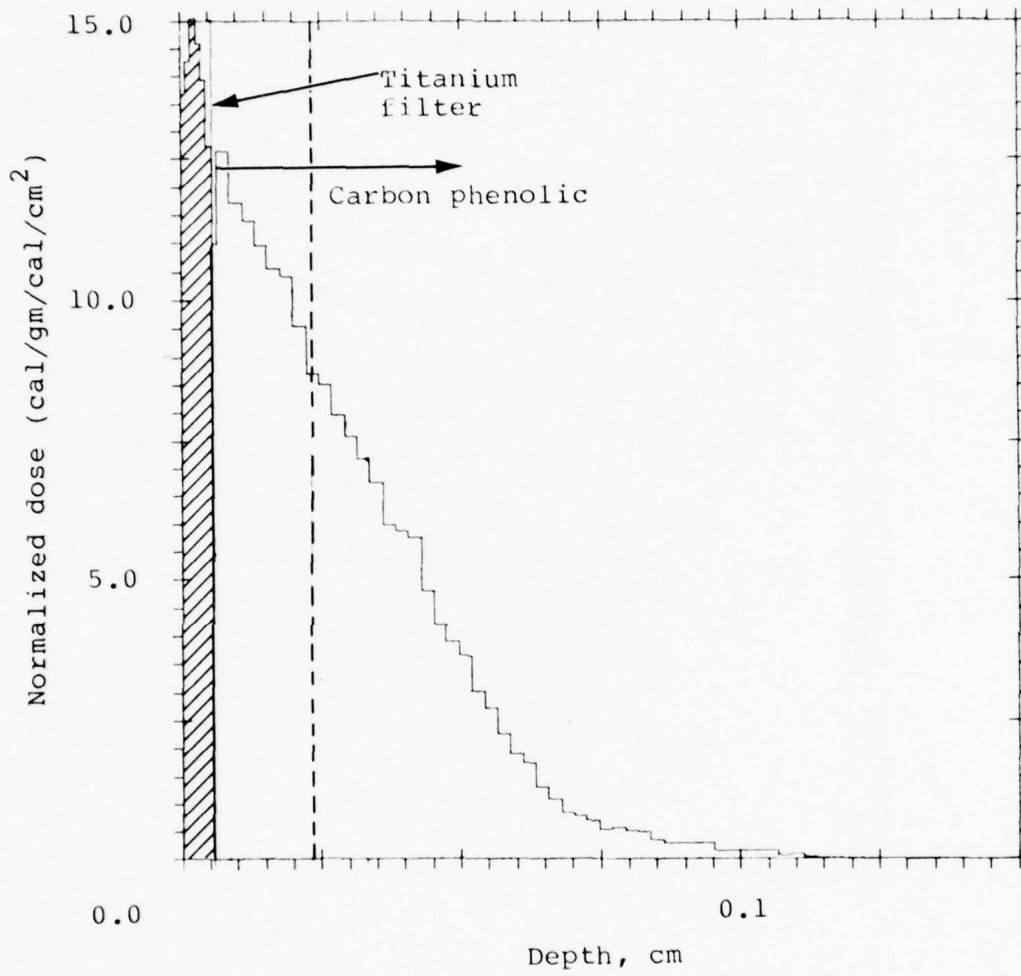


Shot Number 4368

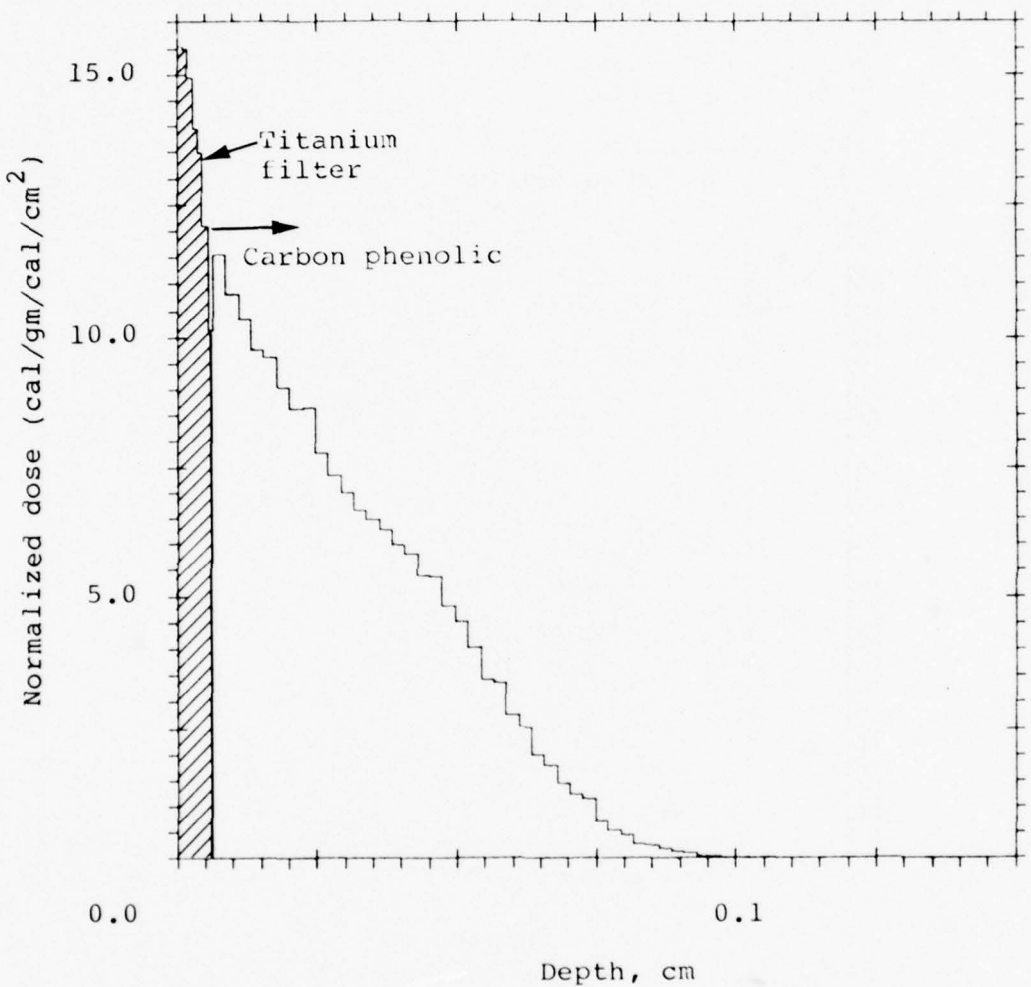


A-2

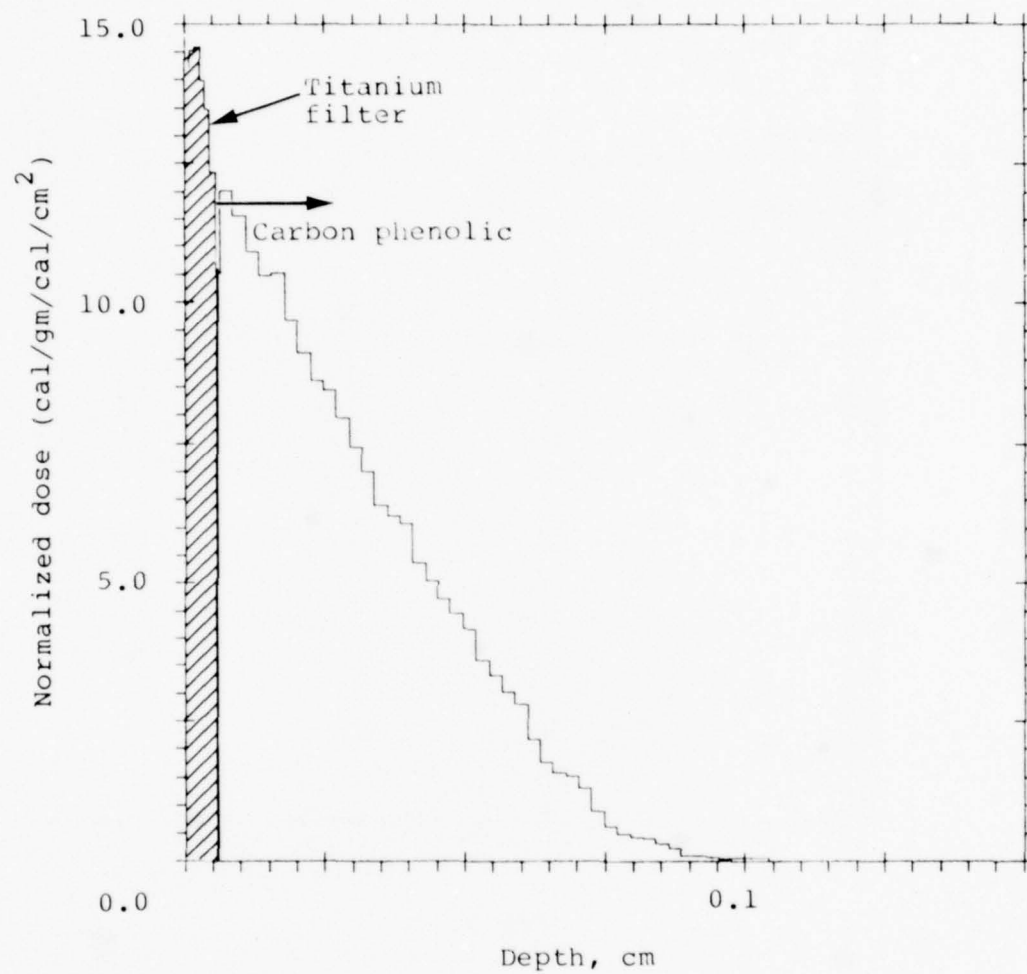
Shot Number 4372

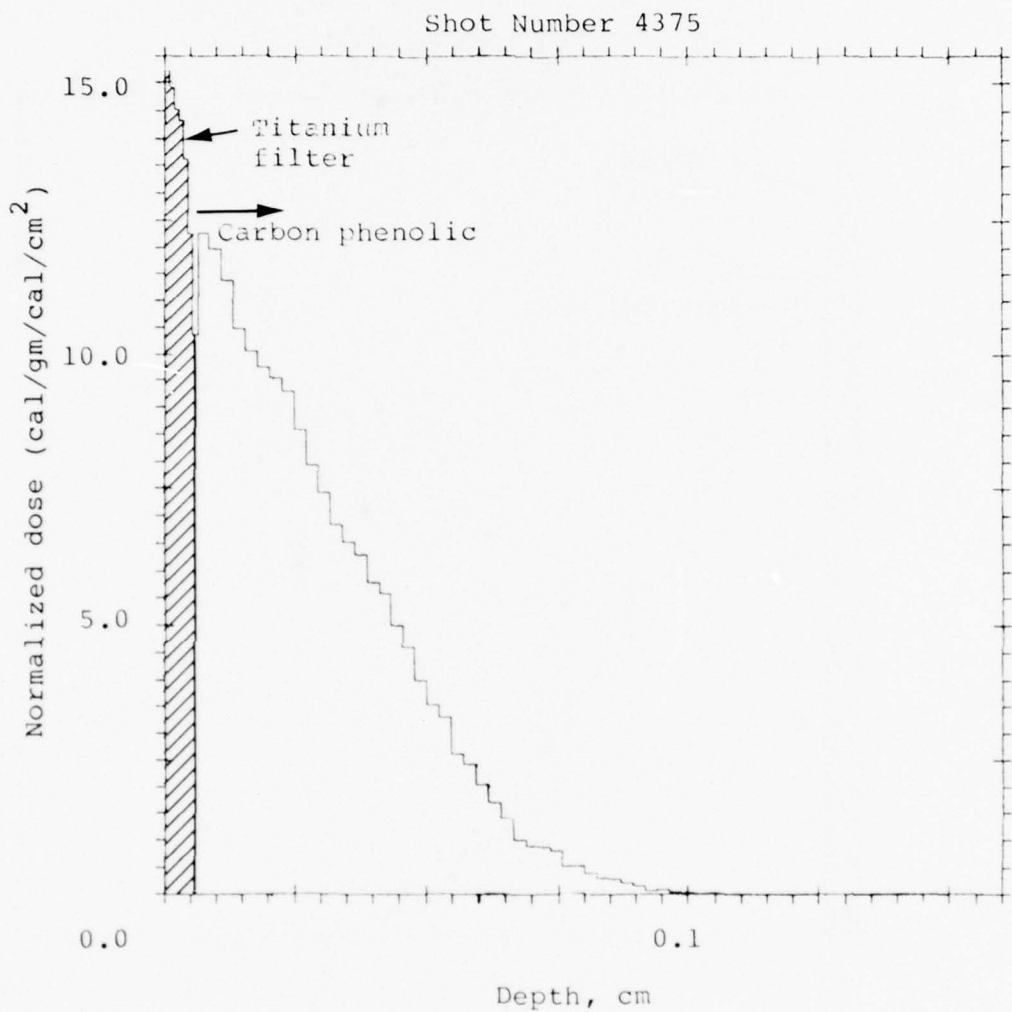


Shot Number 4373

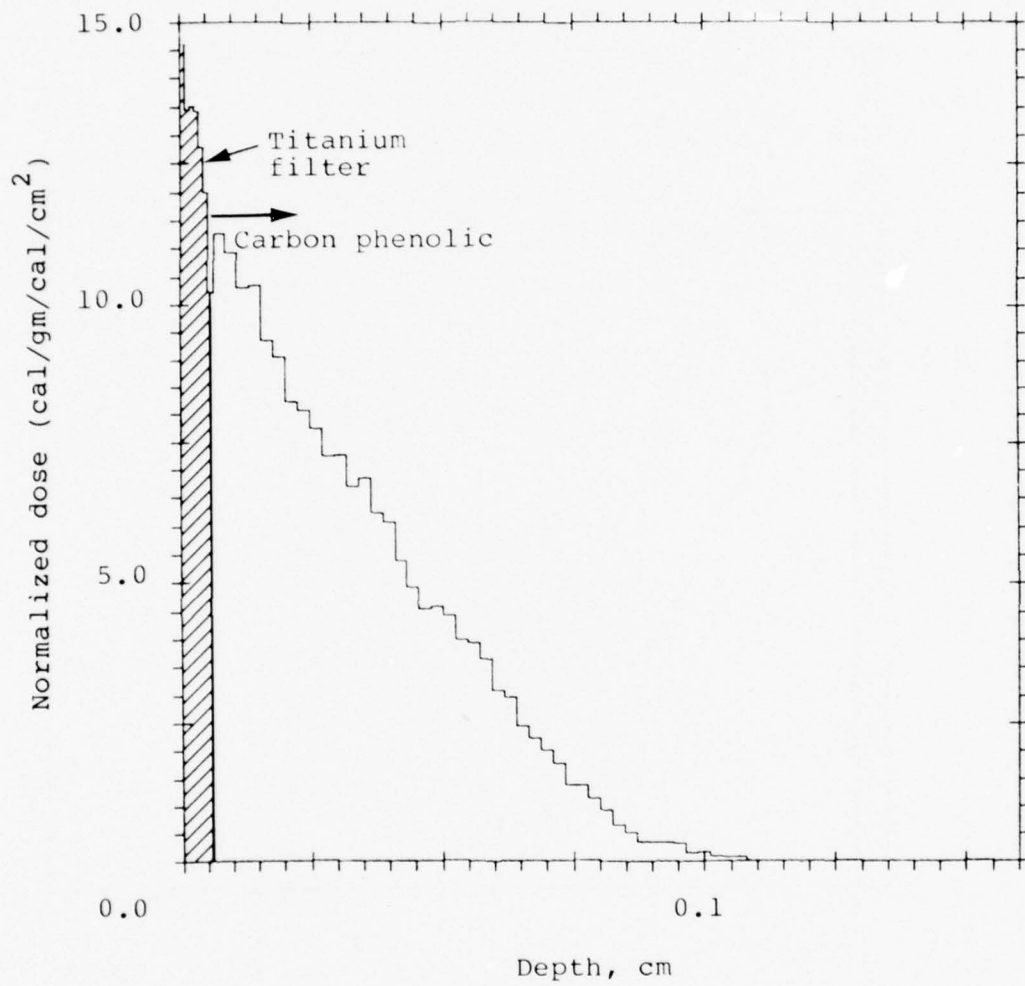


Shot Number 4374



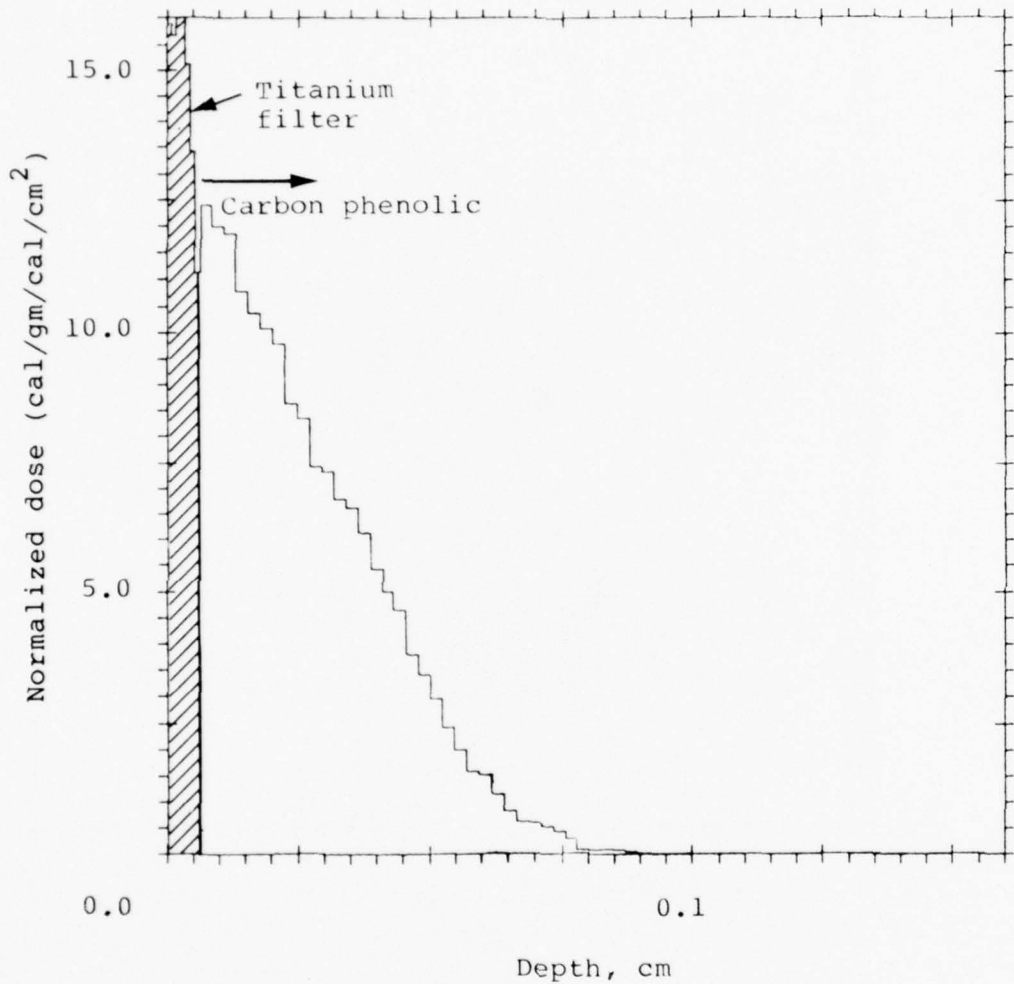


Shot Number 4376

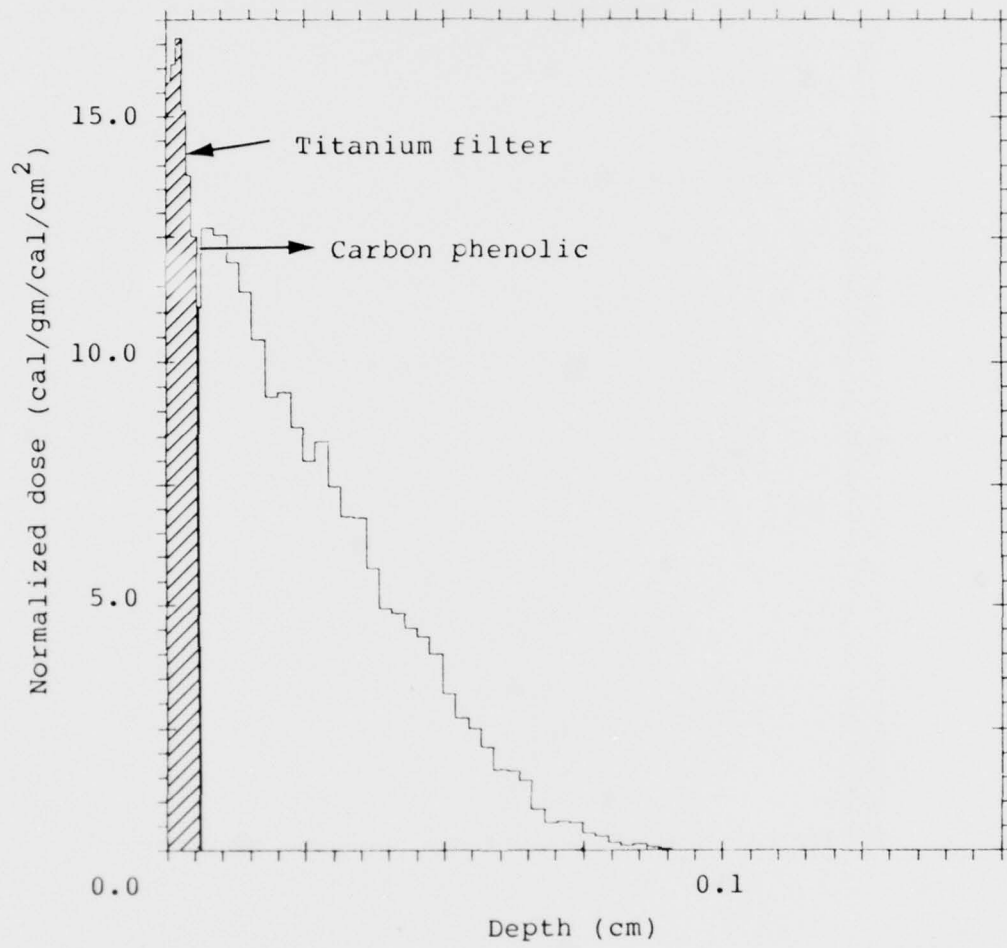


A-7

Shot Number 4378

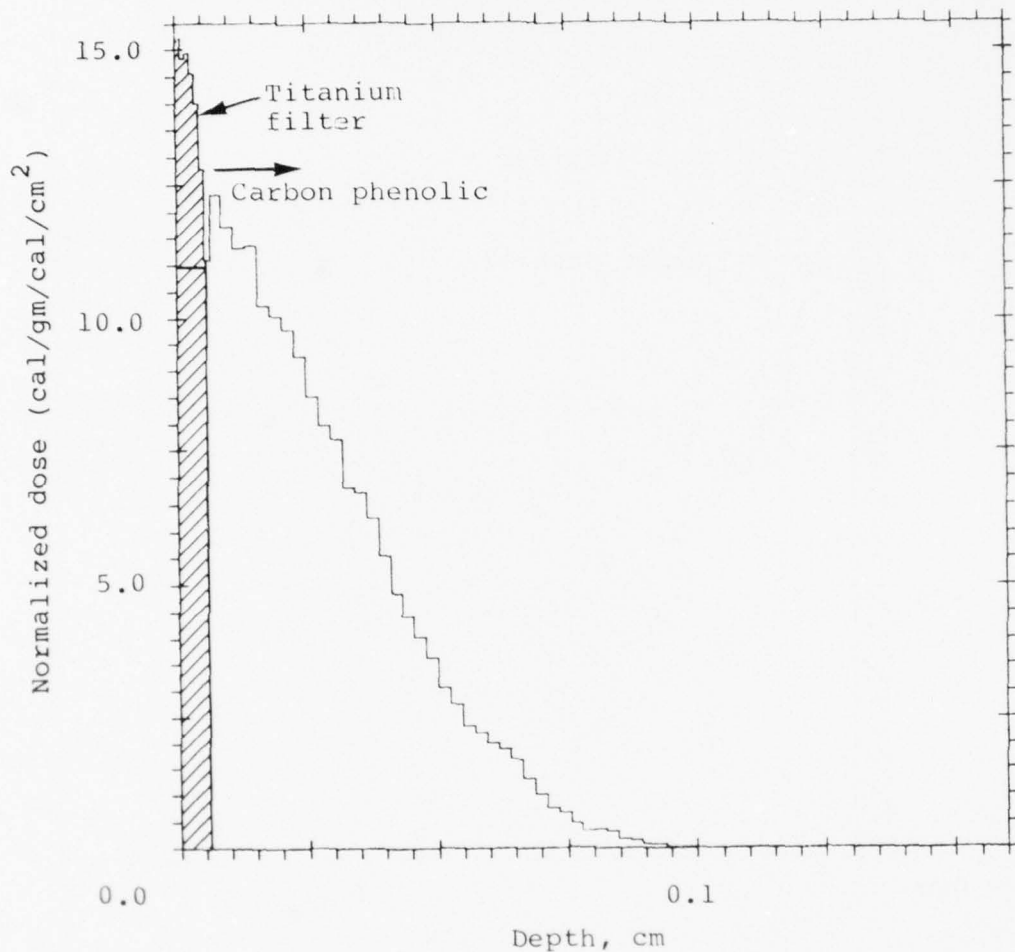


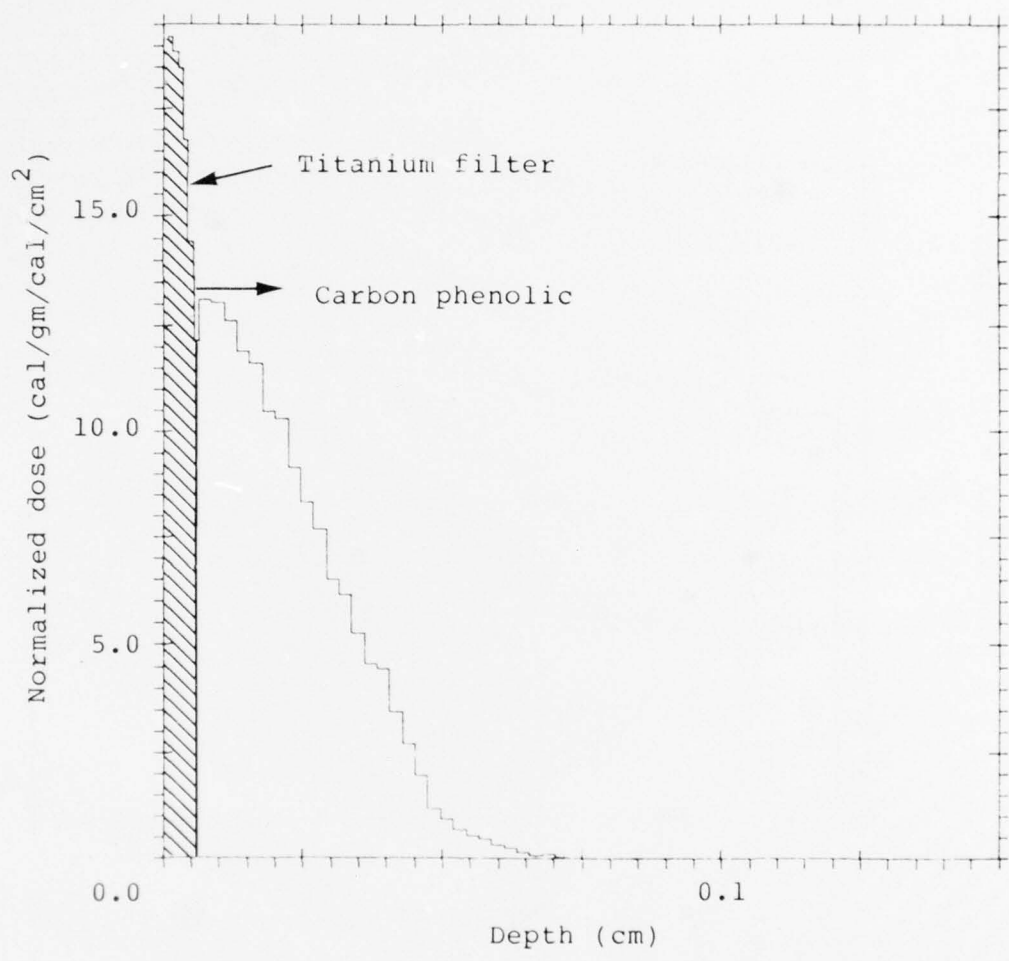
Shot Number 4379



A-9

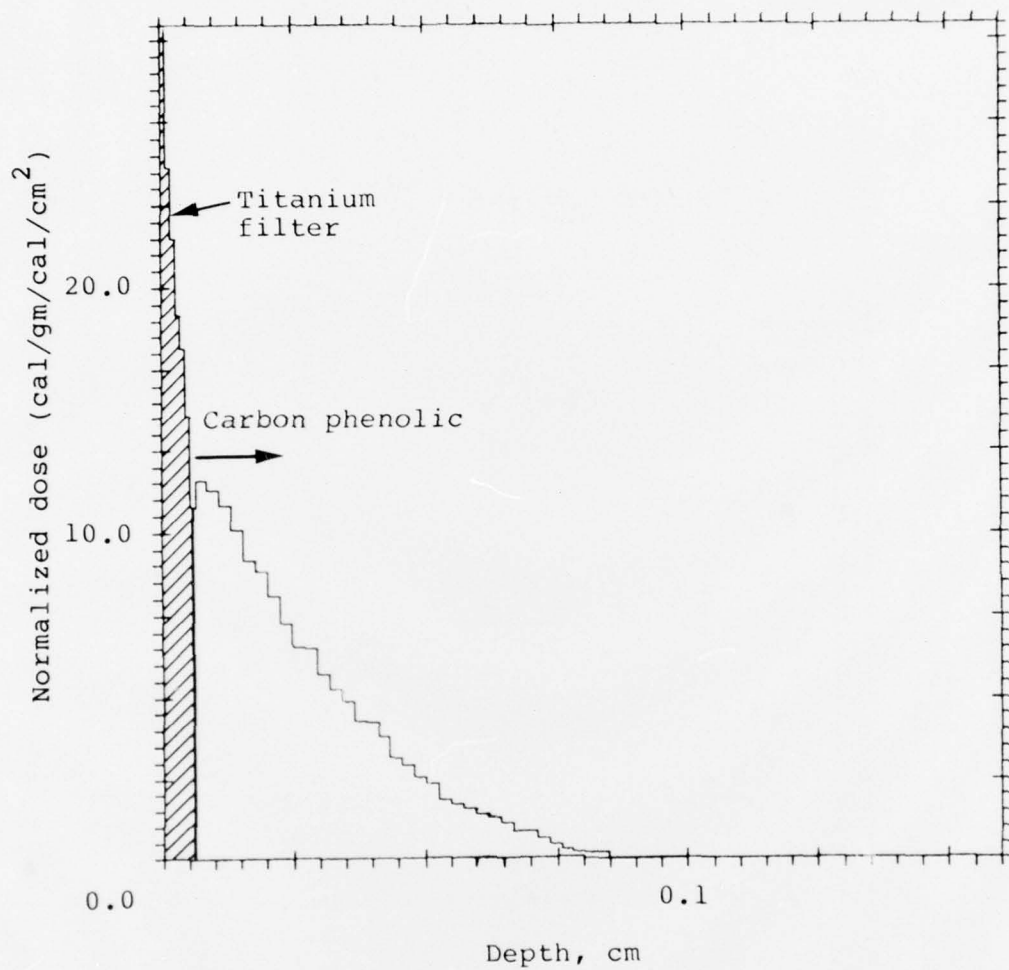
Shot Number 4380





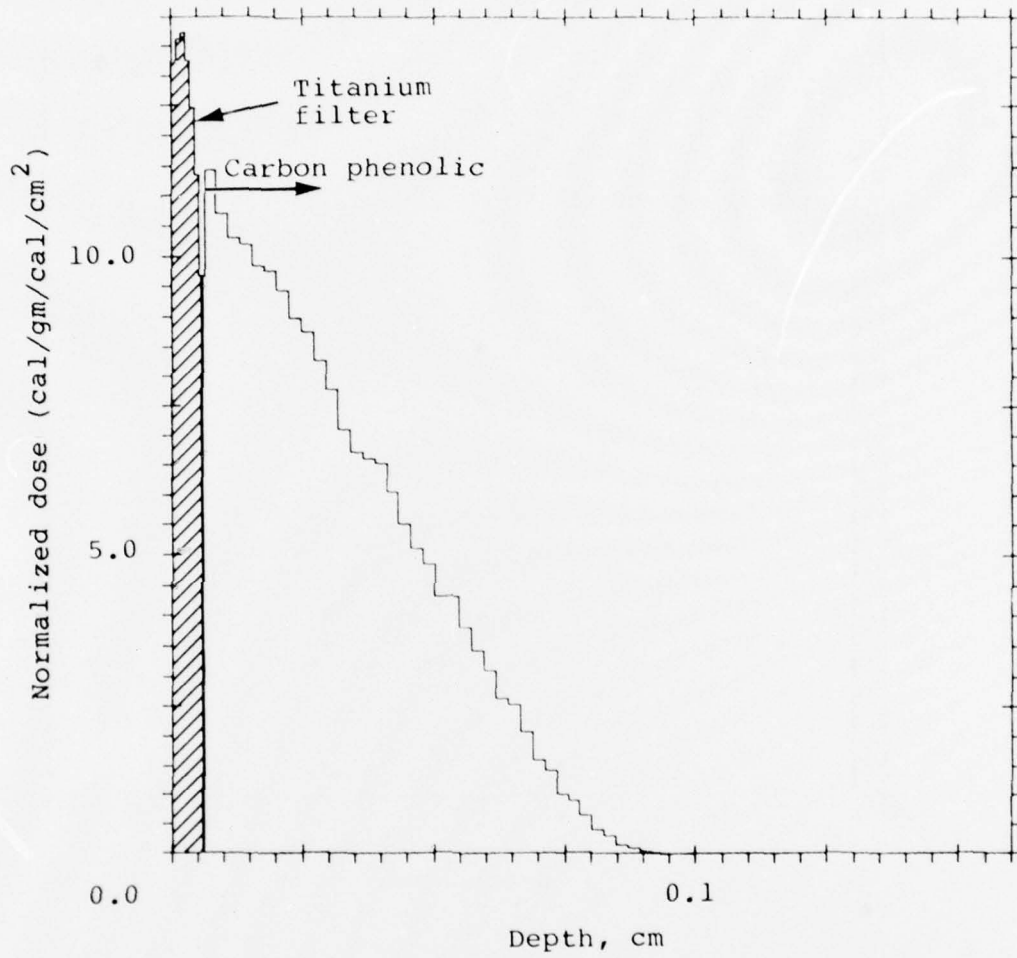
A-11

Shot Number 4382



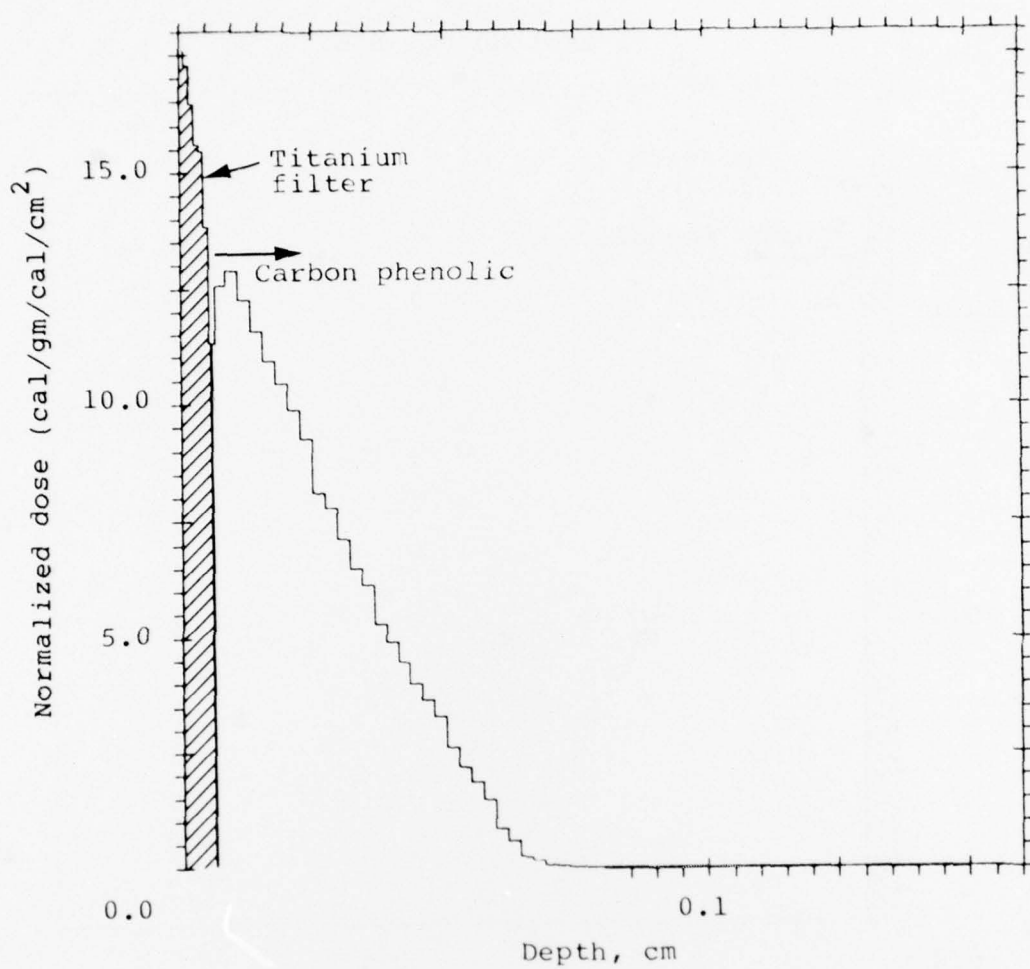
A-12

Shot Number 4384

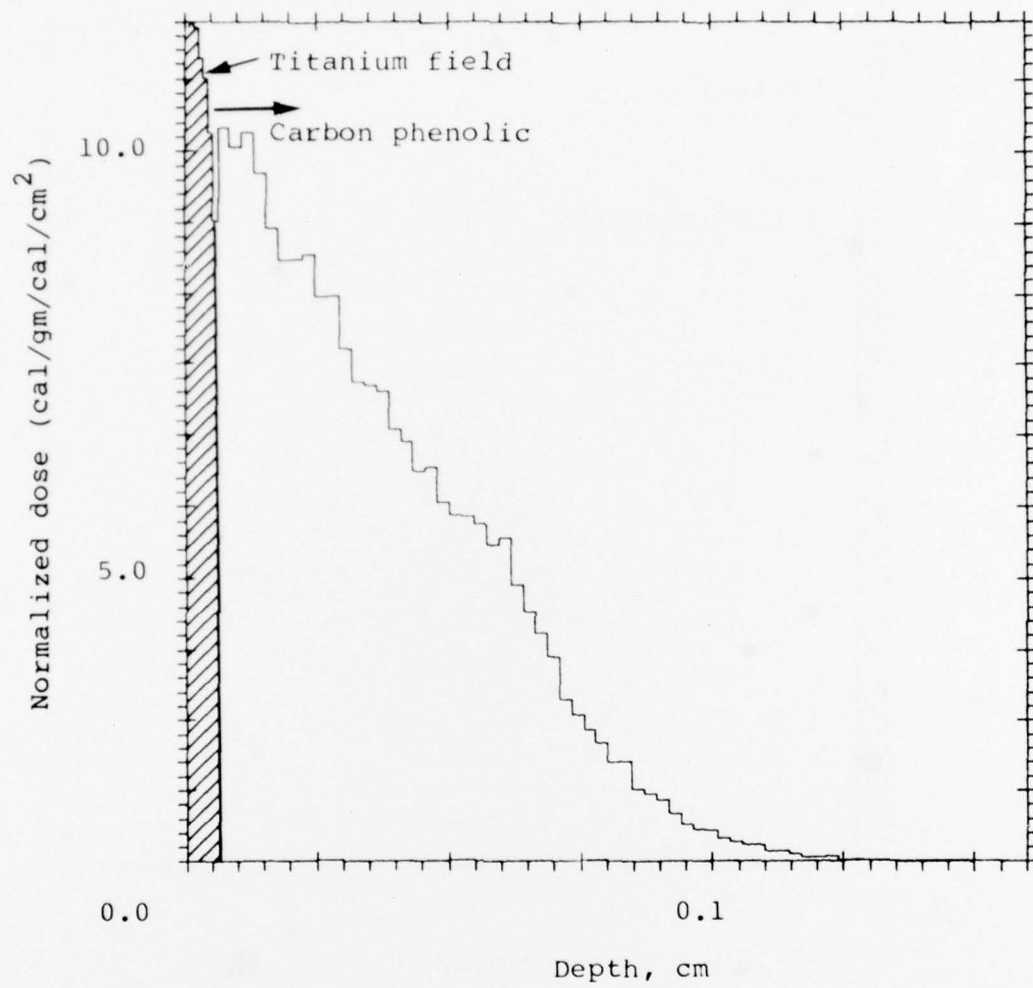


A-13

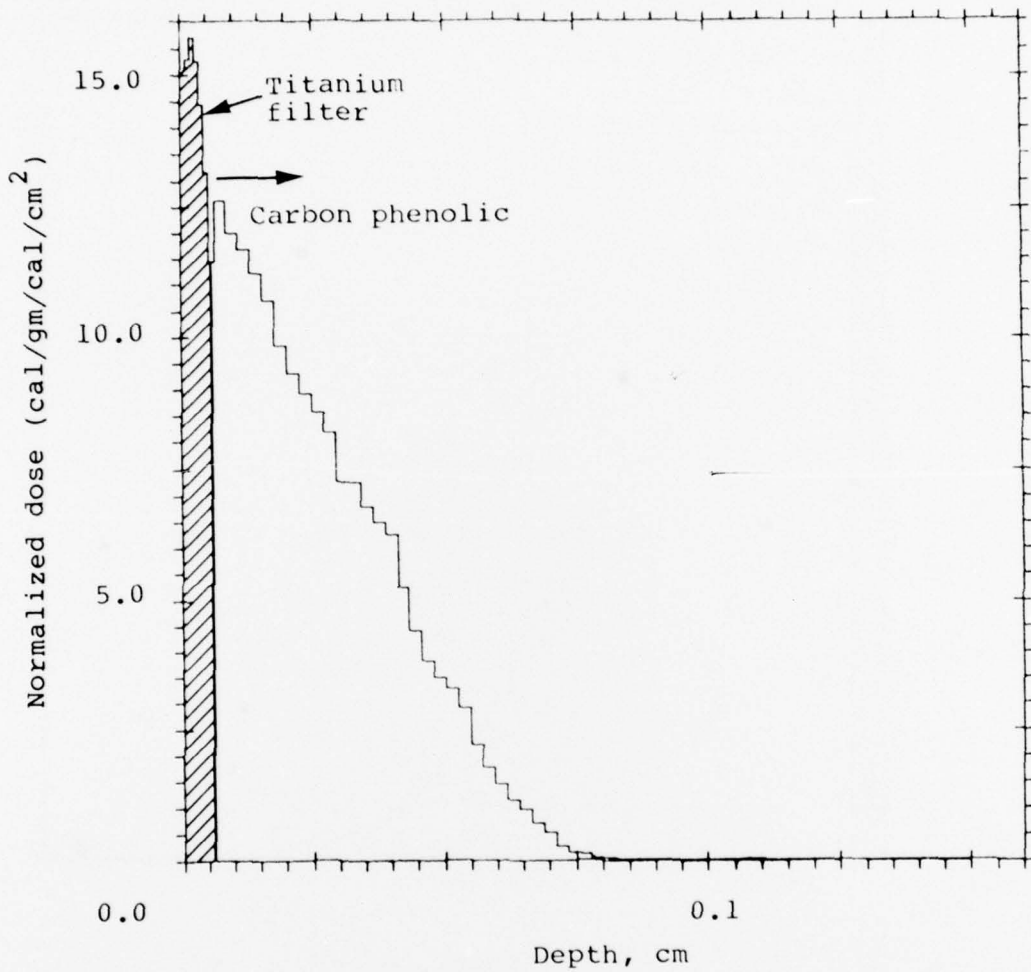
Shot Number 4385



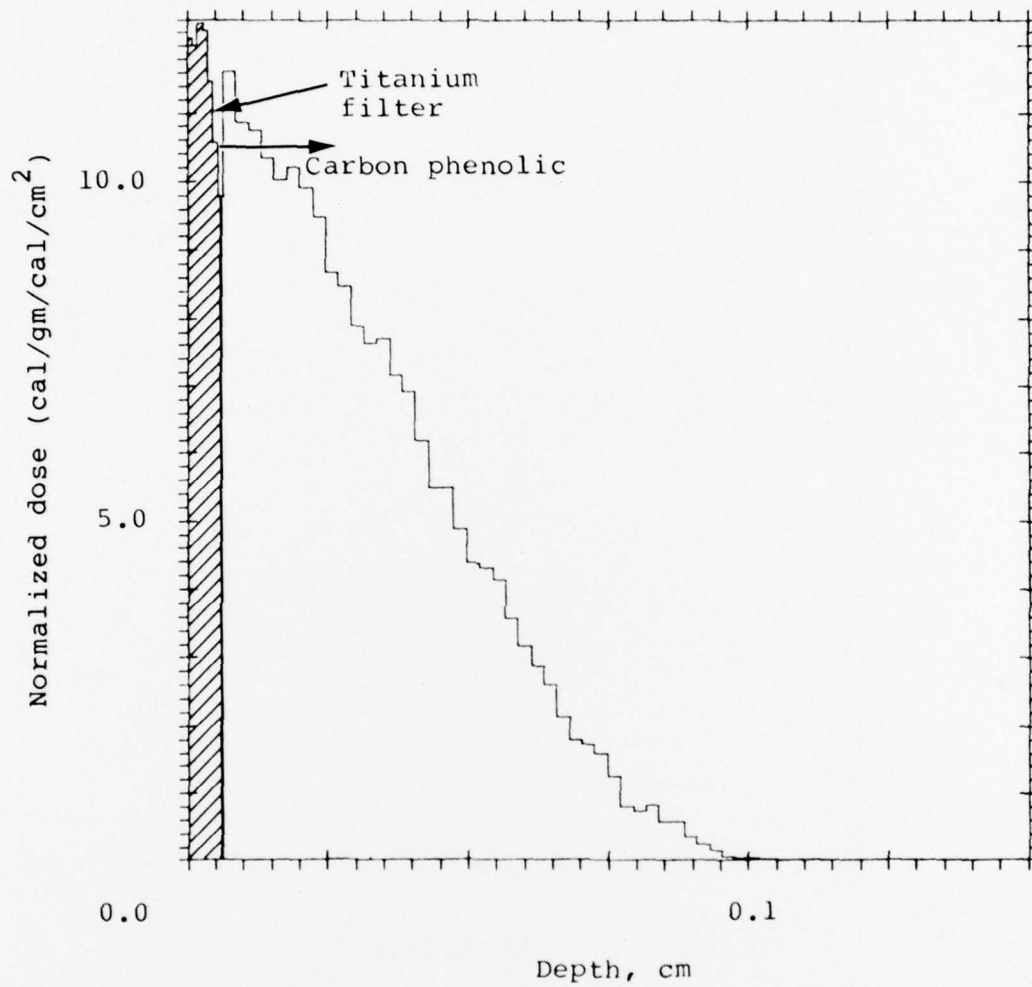
Shot Number 4386

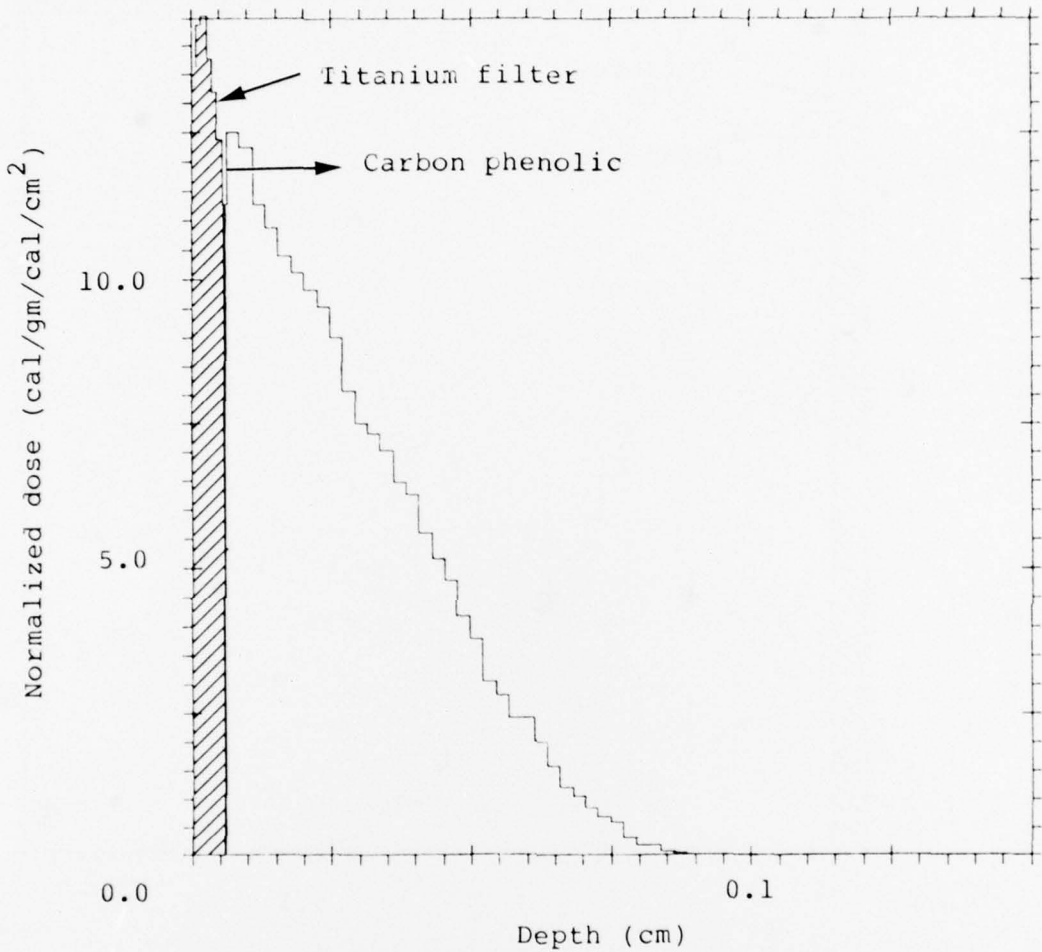


Shot Number 4387

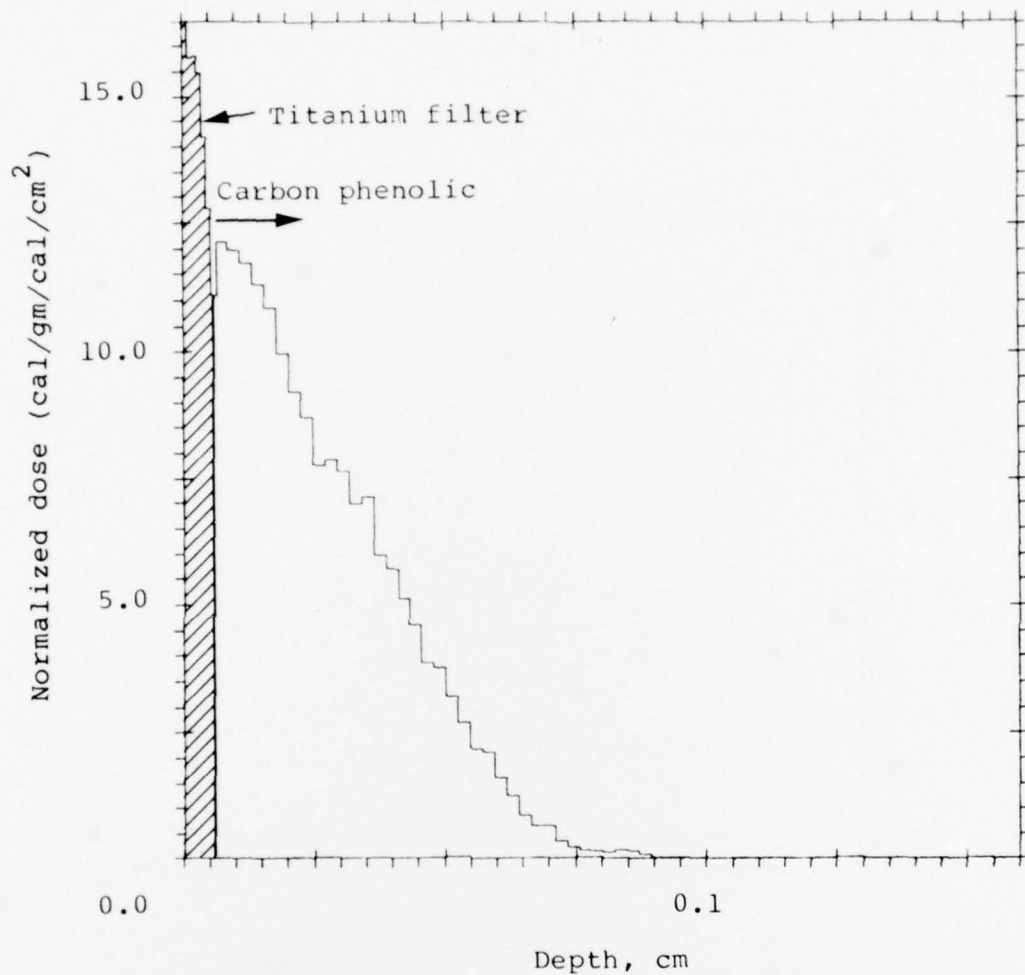


Shot Number 4389



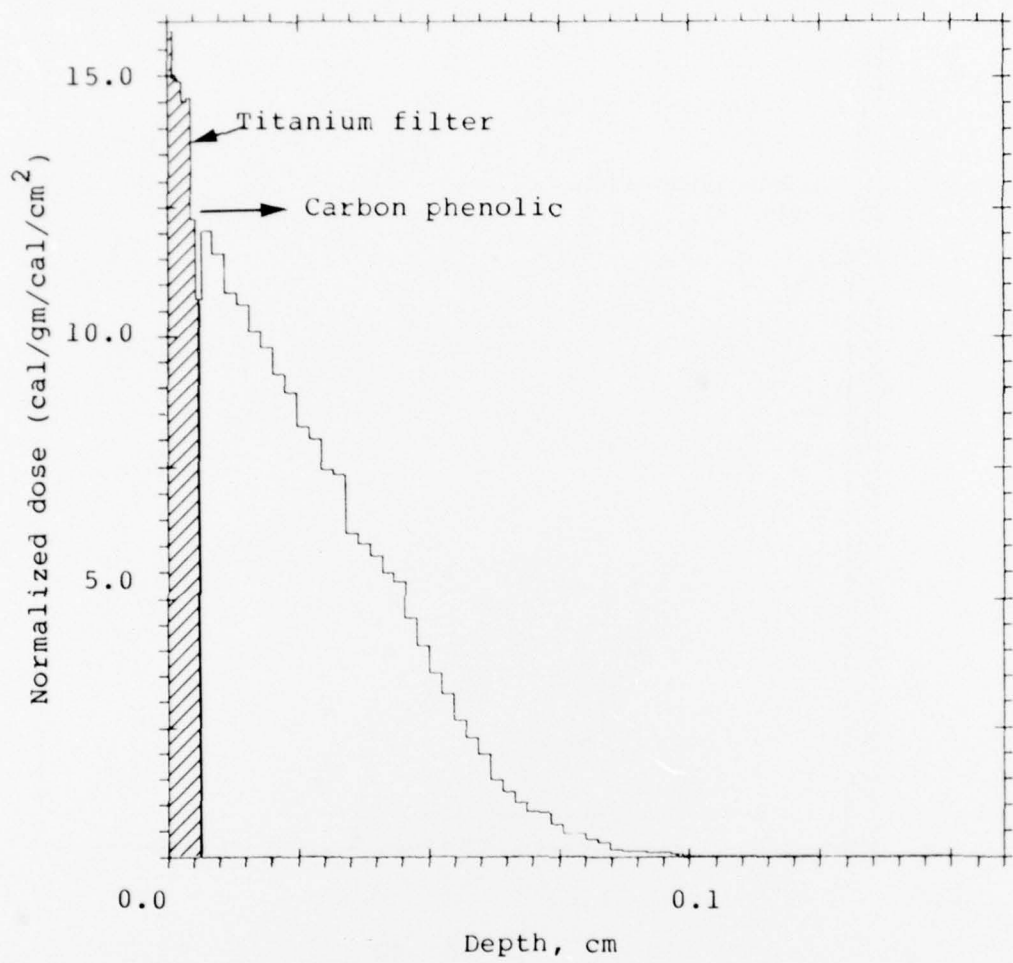


Shot Number 4394

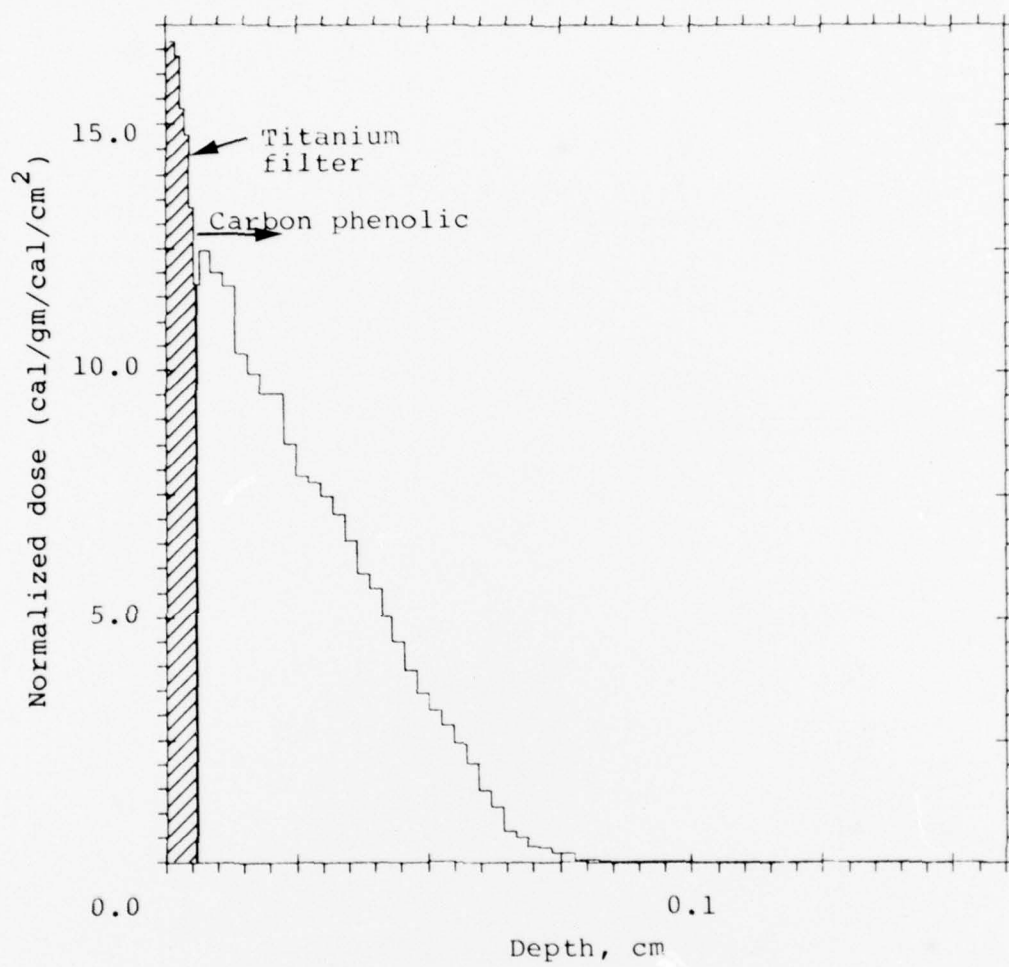


A-19

Shot Number 4395



Shot Number 4396



## DISTRIBUTION LIST

### DEPARTMENT OF DEFENSE

Assistant to the Secretary of Defense  
ATTN: Executive Assistant

Defense Advanced Rsch. Proj. Agency  
ATTN: TIO

Defense Documentation Center  
12 cy ATTN: DD

Defense Intelligence Agency  
ATTN: DT-1B  
ATTN: DT-2

Defense Nuclear Agency  
ATTN: STSP  
ATTN: DOST  
4 cy ATTN: TITL  
3 cy ATTN: SPAS

Field Command  
Defense Nuclear Agency  
ATTN: FCPR

Field Command  
Defense Nuclear Agency  
ATTN: FCPRL

Joint Chiefs of Staff  
ATTN: J-5, Nuclear Division

Joint Strat. Tgt. Planning Staff  
ATTN: JPTM  
ATTN: JLW-2

NATO School (SHAPE)  
ATTN: U.S. Documents Officer

Under Secy. of Def. for Rsch. & Engrg.  
ATTN: Strategic & Space Systems (OS)

### DEPARTMENT OF THE ARMY

BMD Advanced Technology Center  
Department of the Army  
ATTN: ATC-M

BMD Program Office  
Department of the Army  
ATTN: Technology Division

Deputy Chief of Staff for Ops. & Plans  
Department of the Army  
ATTN: DAMO-SSN

Deputy Chief of Staff for Rsch. Dev. & Acq.  
Department of the Army  
ATTN: DAMA-CSS-N

Harry Diamond Laboratories  
Department of the Army  
ATTN: DELHD-RC  
ATTN: DELHD-N-RBH

U.S. Army Ballistic Research Labs  
ATTN: DRDAR-BL, R. Eichelberger

### DEPARTMENT OF THE ARMY (Continued)

U.S. Army Material & Mechanics Rsch. Ctr.  
ATTN: DRXMR-HH

U.S. Army Materiel Dev. & Readiness Cmd.  
ATTN: DRCDE-D

U.S. Army Missile R&D Command  
ATTN: DRDMI-XS

### DEPARTMENT OF THE NAVY

Naval Research Laboratory  
ATTN: Code 2627

Naval Sea Systems Command  
ATTN: SEA-0351

Naval Surface Weapons Center  
ATTN: Code K06  
2 cy ATTN: Code K82

Office of the Chief of Naval Operations  
ATTN: OP 604

Strategic Systems Project Office  
Department of the Navy  
ATTN: NSP-272

### DEPARTMENT OF THE AIR FORCE

Air Force Flight Dynamics Laboratory  
ATTN: FXG  
ATTN: FBC

Air Force Geophysics Laboratory  
ATTN: C. Touart

Air Force Materials Laboratory  
ATTN: MXE  
2 cy ATTN: LTM/MBE  
2 cy ATTN: MBC/MXS

Air Force Office of Scientific Research  
ATTN: P. Thurston

Air Force Rocket Propulsion Laboratory  
ATTN: LKCP

Air Force Systems Command  
ATTN: DLW

Air Force Weapons Laboratory  
ATTN: DYV  
ATTN: SUL

Arnold Engineering Development Center, AFSC  
Department of the Air Force  
ATTN: XRRP

Deputy Chief of Staff  
Research, Development & Acq.  
Department of the Air Force  
ATTN: AFRDQ  
ATTN: AFRDQSM

DEPARTMENT OF THE AIR FORCE (Continued)

Foreign Technology Division, AFSC  
ATTN: SDBG

Space & Missile Systems Organization  
Air Force Systems Command  
ATTN: DYS

Space & Missile Systems Organization  
Air Force Systems Command  
ATTN: MNH  
ATTN: MNNR

Space & Missile Systems Organization  
Air Force Systems Command  
ATTN: RSSR  
ATTN: RSS  
ATTN: RST  
7 cy ATTN: RSSE

Strategic Air Command  
Department of the Air Force  
ATTN: XOBM  
ATTN: XPFS

DEPARTMENT OF ENERGY CONTRACTORS

Lawrence Livermore Laboratory  
University of California  
ATTN: L-92, C. Taylor  
ATTN: L-10, H. Kruger

Los Alamos Scientific Laboratory  
ATTN: J. Taylor

Sandia Laboratories  
ATTN: T. Gold

Sandia Laboratories  
ATTN: A. Chabai  
ATTN: R. Clem  
ATTN: D. Rigali

DEPARTMENT OF DEFENSE CONTRACTORS

Acurex Corp.  
ATTN: J. Huntington  
ATTN: C. Powars  
ATTN: C. Nardo

Aerojet Liquid Rocket Co.  
ATTN: R. Jenkins

Aeronautical Rsch. Assoc. of Princeton, Inc.  
ATTN: C. Donaldson

Aerospace Corp.  
ATTN: W. Grabowsky  
ATTN: H. Dyner  
ATTN: D. Nowlan  
ATTN: D. Platus  
ATTN: R. Palmer  
ATTN: D. Geiller  
ATTN: R. Hallse  
ATTN: P. Legendre  
ATTN: M. Gyetvay  
ATTN: W. Portenier  
ATTN: W. Barry  
ATTN: R. Mortensen

DEPARTMENT OF DEFENSE CONTRACTORS (Continued)

Aro, Inc.  
ATTN: G. Norfleet  
ATTN: J. Adams

Avco Research & Systems Group  
ATTN: J. Stevens  
ATTN: W. Broding  
ATTN: A. Pallone  
ATTN: V. Dicristina

The Boeing Company  
ATTN: B. Lempriere

Calspan Corp.  
ATTN: M. Holden

Effects Technology, Inc.  
ATTN: R. Wengler

Fiber Materials, Inc.  
ATTN: M. Subilia

Ford Aerospace & Communications Corp.  
ATTN: A. Demetriades

General Electric Company  
Re-Entry & Environmental Systems Div  
ATTN: B. Maguire  
ATTN: P. Cline

General Electric Company-TEMPO  
Center for Advanced Studies  
ATTN: DASIAC

General Research Corp.  
ATTN: R. Rosenthal

Institute for Defense Analyses  
ATTN: J. Bengston  
ATTN: Classified Library

Ion Physics Corp.  
ATTN: R. Evans

Kaman Sciences Corp.  
ATTN: F. Shelton  
ATTN: T. Meagher

Lockheed Missiles & Space Co., Inc.  
ATTN: R. Au  
ATTN: D. Price  
ATTN: P. Schneider  
ATTN: G. Chruscziel  
ATTN: C. Lee

Lockheed Missiles and Space Co., Inc.  
2 cy ATTN: T. Fortune

Martin Marietta Corp.  
ATTN: L. Kinnaird  
ATTN: R. Cramer

McDonnell Douglas Corp.  
ATTN: G. Fitzgerald  
ATTN: L. Cohen  
ATTN: H. Hurwicz

DEPARTMENT OF DEFENSE CONTRACTORS (Continued)

National Academy of Sciences  
National Materials Advisory Board  
ATTN: D. Groves

Pacific-Sierra Research Corp.  
ATTN: G. Lang

Physical Sciences, Inc.  
ATTN: M. Finsen

Physics International Co.  
ATTN: J. Shea  
ATTN: K. Triebes

Prototype Development Associates, Inc.  
ATTN: J. Dunn  
3 cy ATTN: C. Thacker

R & D Associates  
ATTN: F. Field  
ATTN: C. MacDonald  
ATTN: P. Rausch  
ATTN: R. Ross

Science Applications, Inc.  
ATTN: J. Warner

Science Applications, Inc.  
ATTN: K. Kratsch  
ATTN: J. Courtney  
ATTN: L. Dunbar

DEPARTMENT OF DEFENSE CONTRACTORS (Continued)

Science Applications, Inc.  
ATTN: C. Kyriss  
ATTN: A. Martellucci

Southern Research Institute  
ATTN: C. Pears

Spectron Development Labs, Inc.  
ATTN: T. Lee

SRI International  
ATTN: D. Curran  
ATTN: G. Abrahamson

Systems, Science & Software, Inc.  
ATTN: G. Gurtman

TRW Defense & Space Sys. Group  
ATTN: I. Alber  
ATTN: T. Williams  
ATTN: D. Baer  
ATTN: W. Wood  
ATTN: R. Myer

TRW Defense & Space Sys. Group  
ATTN: V. Blankenship  
ATTN: E. Allen  
ATTN: L. Berger  
ATTN: E. Wong  
ATTN: W. Polich

